

Discovery of 1-Butyl-3-chloro-4-(4-phenyl-1-piperidinyl)-(1*H*)-pyridone (JNJ-40411813): A Novel Positive Allosteric Modulator of the Metabotropic Glutamate 2 Receptor

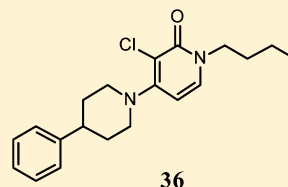
José María Cid,^{*,†} Gary Tresadern,[†] Guillaume Duvey,^{1,○} Robert Lütjens,^{1,○} Terry Finn,¹ Jean-Philippe Rocher,¹ Sonia Poli,¹ Juan Antonio Vega,[†] Ana Isabel de Lucas,[†] Encarnación Matesanz,[†] María Lourdes Linares,[†] José Ignacio Andrés,[†] Jesús Alcazar,[†] José Manuel Alonso,[†] Gregor J. Macdonald,[‡] Daniel Oehlich,[‡] Hilde Lavreysen,[§] Abdelah Ahnaou,[§] Wilhelmus Drinkenburg,[§] Claire Mackie,^{||} Stefan Pype,[#] David Gallacher,[∇] and Andrés A. Trabanco[†]

[†]Neuroscience Medicinal Chemistry, Janssen Research & Development, Janssen-Cilag S.A., C/Jarama 75, 45007 Toledo, Spain

[‡]Neuroscience Medicinal Chemistry, [§]Neuroscience Biology, ^{||}Discovery ADME/Tox, ¹Molecular Sciences, [#]Project Management Office, [∇]Translational Sciences, Janssen Research & Development, Turnhoutseweg 30, B-2340, Beerse, Belgium

[○]Addex Therapeutics, 12 Chemin des Aulx, 1228 Plan-les-Ouates, Geneva, Switzerland

ABSTRACT: We previously reported the discovery of 4-aryl-substituted pyridones with mGlu2 PAM activity starting from the HTS hit **5**. In this article, we describe a different exploration from **5** that led to the discovery of a novel subseries of phenylpiperidine-substituted pyridones. The optimization strategy involved the introduction of different spacers between the pyridone core and the phenyl ring of **5**. The fine tuning of metabolism and hERG followed by differentiation of advanced leads that were identified on the basis of PK profiles and in vivo potency converged on lead compound **36** (JNJ-40411813). Full in vitro and in vivo profiles indicate that **36** displayed an optimal interplay between potency, selectivity, favorable ADMET/PK and cardiovascular safety profile, and central EEG activity. Compound **36** has been investigated in the clinic for schizophrenia and anxious depression disorders.



mGlu2 PAM EC₅₀ = 147 nM
 mGlu2 PAM E_{MAX} = 273%

Phase 2 clinical trials

INTRODUCTION

Glutamate is the major excitatory neurotransmitter in the central nervous system (CNS) of vertebrates and elicits and modulates synaptic responses in the CNS by activating ionotropic glutamate (iGlu) receptors and metabotropic glutamate (mGlu) receptors.¹ To date, eight mGlu receptor subtypes and multiple splice variants have been cloned and classified into three groups based on sequence homology, pharmacological profile, and preferential signal transduction pathways:^{2,3} group I (mGlu1 and mGlu5), group II (mGlu2 and mGlu3), and group III mGlu receptors (mGlu4, mGlu6, mGlu7, and mGlu8). Pharmaceutical companies and academic groups have primarily focused on the pharmacology and development of ligands acting at group I (mGlu1 and 5) and II (mGlu2 and 3) receptors, whereas group III (mGlu4, 6, 7, and 8) receptors have started to attract more attention recently.^{4,5} Group II mGlu receptors, which are located presynaptically in the periphery of the synapse, reduce glutamatergic transmission in brain regions such as the prefrontal cortex and hippocampus,⁶ where excessive glutamatergic transmission has been implicated in the pathophysiology of anxiety and schizophrenia. Mixed mGlu2/3 orthosteric agonists such as (+)-2-aminobicyclo[3.1.0]hexane-2,6-dicarboxylic acid **1** (LY354740) have shown activity in a wide range of preclinical animal models of anxiety and schizophrenia.⁷ Animal studies

with the NMDA receptor antagonist phencyclidine (PCP) and mixed mGlu2/3 receptor agonists provided the first insights that revealed that mGlu2 receptor activation may represent a novel target for the treatment of schizophrenia.^{8,9} In its first clinical trial, (1*R*,4*S*,5*S*,6*S*)-2-thiabicyclo[3.1.0]hexane-4,6-dicarboxylic acid 4-[(2*S*)-2-amino-4-(methylthio)-1-oxobutyl]-amino-2,2-dioxide monohydrate **2** (LY2140023), a prodrug of (-)-(1*R*,4*S*,5*S*,6*S*)-4-amino-2-sulfonylbicyclo[3.1.0]hexane-4,6-dicarboxylic acid **3** (LY404039), demonstrated improvements in positive and negative symptoms compared to placebo in schizophrenic patients.¹⁰ However, these positive data could not be confirmed in follow-up studies,^{11,12} and very recently, Eli Lilly and Co. announced the decision to stop the phase III development of **2** for the treatment of patients suffering from schizophrenia based on efficacy results.¹³

On the other hand, the anxiolytic potential of **1** was confirmed in healthy human volunteers, showing activity in fear-potentiated startle and panic induction after CO₂ challenge.¹⁴

Despite the interesting findings, there remain hurdles in developing clinically useful agonists. First, all agonists identified so far lack mGlu2 receptor subtype selectivity and also act on

Received: March 28, 2014

Published: July 17, 2014

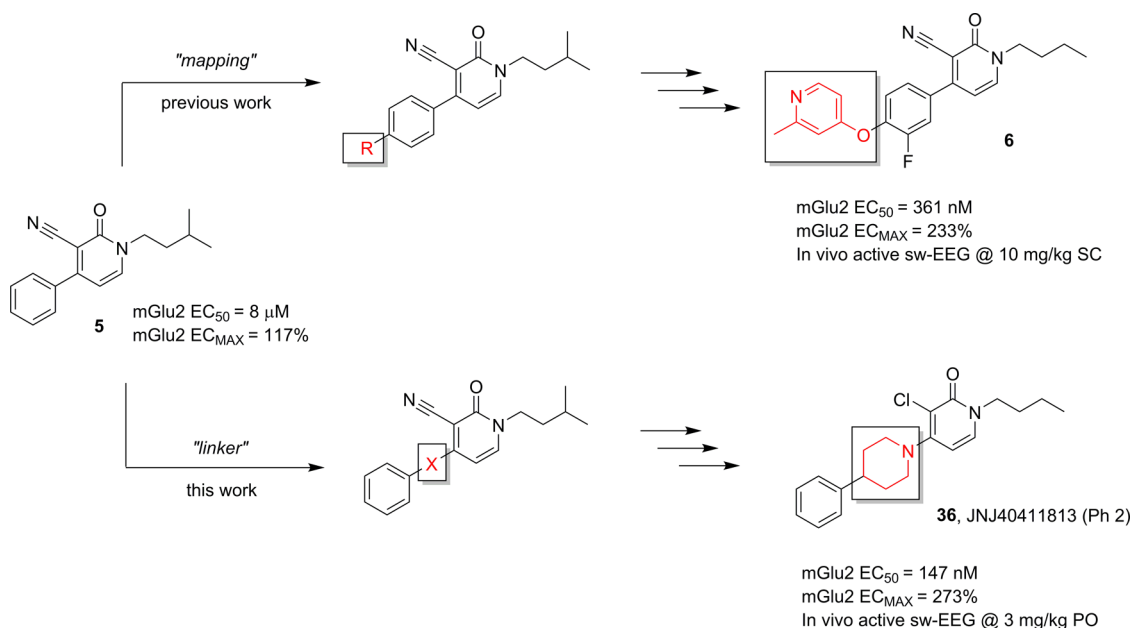
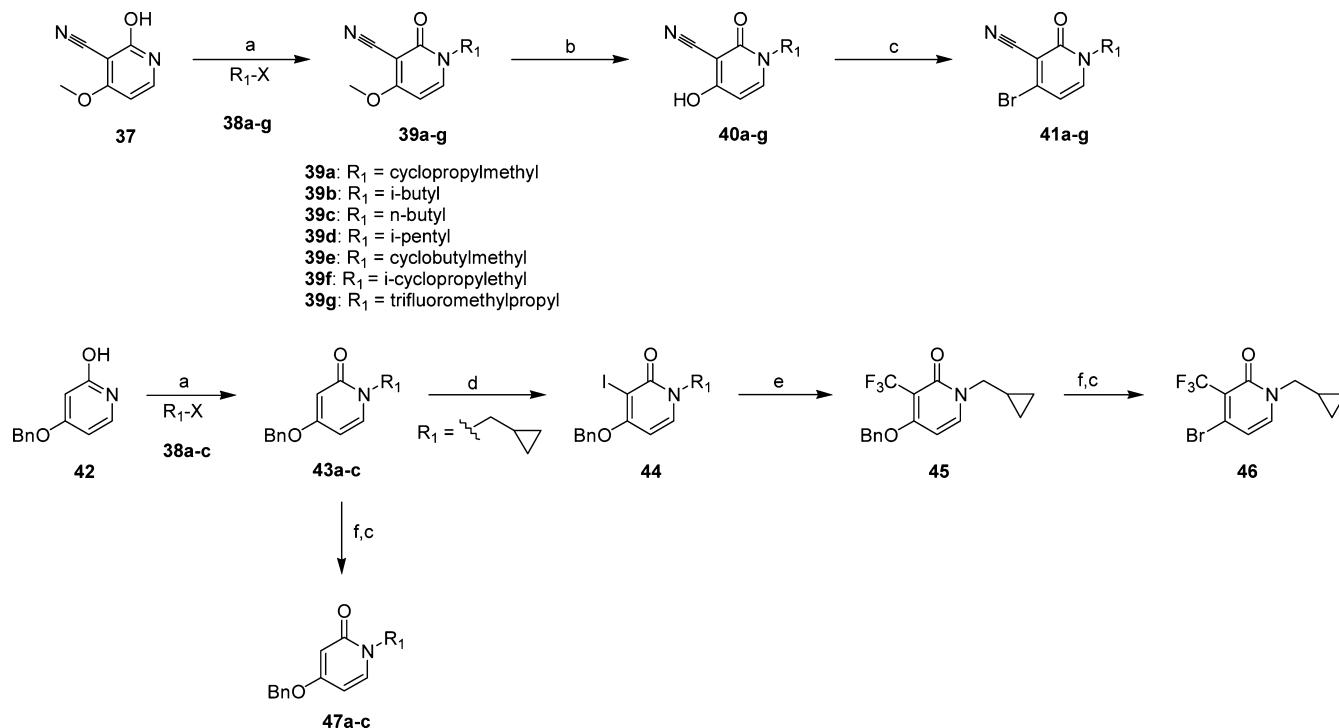


Figure 1. Strategies followed for the exploration of HTS hit 5.

Scheme 1. Preparation of 4-Bromopyridone Building Blocks 41a–g, 46, and 47a–c^a



^aReagents and conditions: (a) K₂CO₃, MeCN, 100 °C, 16 h; (b) NaOH, H₂O, reflux, 18 h; (c) POBr₃, DMF, 110 °C, 1–3 h; (d) NIS, AcOH, rt, 1 h; (e) FSO₂CF₂CO₂Me, CuI, DMF, 100 °C, 5 h; (f) H₂, Pd/C, EtOH, rt, 2 h.

the mGlu3 receptor. It has been shown that the mGlu2, and not the mGlu3 receptor, mediates the actions of the mGlu2/3 receptor agonists (1*S*,2*R*,5*R*,6*R*)-2-amino-4-oxabicyclo[3.1.0]hexane-2,6-dicarboxylic acid (LY379268) and 3 in mouse models predictive of antipsychotic activity.^{15,16} Second, the development of tolerance by group II mGlu receptor agonists has been observed in several rodent behavioral models.¹⁷

Receptor activation with positive allosteric modulators (PAMs), which act via alternative allosteric site(s), offers

several advantages.¹⁸ Allosteric molecules are likely to be less polar and to have improved CNS penetration, as they do not require amino-acid functional groups for activity at the orthosteric site. Furthermore, the less conserved nature of allosteric site(s) can allow for improved mGlu receptor subtype selectivity. Finally, allosteric modulators exert their effects only in the presence of endogenous glutamate, so they may be less prone to cause receptor desensitization,^{19,20} and they respond to physiological glutamate fluctuations. Given these potential

advantages, the number of reported mGlu2 receptor-selective PAMs has increased in recent years.^{21,22} Some of these compounds have been extensively characterized in a number of animal models, providing preclinical proof of concept that PAMs can mimic the effects of orthosteric agonists.^{23–32}

To date, two mGlu2 PAM molecules have advanced into clinical trials: **4** (AZD8529) from AstraZeneca AB (structure undisclosed) and **36**^{33–35} (also known as ADX71149 in Figure 1) from Janssen Pharmaceuticals and Addex Therapeutics. On January 2011, the originating company announced the discontinuation of **4** phase IIa POC study in schizophrenic patients due to lack of efficacy.^{36,37} More promisingly, it has been disclosed that, in an exploratory phase IIa study in schizophrenia, **36** proved to meet the primary objectives of safety and tolerability. Moreover, patients treated with antipsychotics who experience residual negative symptoms were identified as the subgroup of patients who may potentially benefit from add-on treatment with **36**, although this is yet to be established in a formal proof-of-concept study.^{38,39}

Additionally, a phase II POC study with **36** as adjunctive therapy in patients with major depressive disorder (MDD) with significant anxiety symptoms has been completed.⁴⁰ Overall, **36** was well-tolerated, and treatment emergent adverse events reported were similar to those seen in previous clinical studies. On the basis of a preliminary analysis of the primary efficacy end point, the 6-Item Hamilton Anxiety Subscale (HAM-A6), **36** did not meet the criterion for efficacy signal detection versus placebo. Despite a lack of signal on the primary outcome measure, treatment with **36** showed efficacy signals on several anxiety measures (HDRS17 anxiety somatization factor, IDS-C30 anxiety subscale) and on all depression measures (HDRS17, HAM-D6, and IDS-C30).⁴¹ Although efficacy signals were evident, the data overall does not support the further development of **36** in anxious depression. Further exploration of **36** in other indications remains of potential interest.

We have recently reported on a series of pyridones derived from the optimization of the HTS hit **5** that led to the identification of compound **6**.^{29,42} Compound **6** combined moderate in vitro activity, good pharmacokinetic profile, and robust in vivo activity. The optimization strategy involved the introduction of a variety of substituents in the *para* position of the phenyl ring in hit **5** (Figure 1; mapping). Herein, we report on a new optimization strategy consisting of the exploration of different spacers (Figure 1; linker) between the pyridone core and the aromatic ring in hit **5**.^{43,44} This strategy resulted in the identification of our clinical lead, **36**, whose identification path, SAR, and a general overview of its pharmacological profile are reported herein.

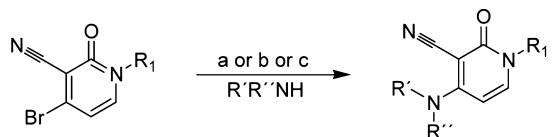
CHEMISTRY

The synthesis of the 1,3,4-trisubstituted 2-pyridone derivatives **6–36**^{32,42} is outlined in Schemes 1–5. The key bromopyridone intermediates, **41a–g**, **46**, and **47a–c**, were prepared as shown in Scheme 1. Treatment of 2-hydroxypyridine derivative **37** with the required alkyl halides **38a–g** afforded the *N*-alkylated 2-pyridones **39a–g**. Subsequent cleavage of the methyl ether followed by treatment of the resulting hydroxypyridones **40a–g** with POBr₃ yielded the intermediates **41a–g**. In a similar way, intermediates **43a–c** were obtained by alkylation of the 2-hydroxy-4-benzyloxy pyridine **42** with the corresponding alkyl halides **38a–c**. Iodination of compound **43a** (R¹ = cyclopropylmethyl) with *N*-iodosuccinimide (NIS) afforded the 3-

iodopyridone **44**, which was subsequently converted into the corresponding 3-trifluoromethylpyridone **45** by treatment with the nucleophilic trifluoromethyl-copper complex generated from fluorosulfonyldifluoroacetate. Finally, cleavage of the benzyl ether in intermediates **43a–c** and **45** followed by reaction with POBr₃ under thermal conditions yielded the target intermediates **47a–c** and **46**, respectively.

The synthesis of the final compounds **8–21**, **26–29**, **31**, **32**, and **34** is illustrated in Scheme 2. Treatment of bromopyridone

Scheme 2. Synthesis of the Final Compounds 8–21, 26–29, 31, 32, and 34^a



41a: R₁ = cyclopropylmethyl; R₂ = cyano

41b: R₁ = *i*-butyl; R₂ = cyano

41c: R₁ = *n*-butyl; R₂ = cyano

41d: R₁ = *i*-pentyl; R₂ = cyano

41e: R₁ = cyclobutylmethyl; R₂ = cyano

41f: R₁ = *i*-cyclopropylethyl; R₂ = cyano

41g: R₁ = trifluoromethylpropyl; R₂ = cyano

46: R₁ = cyclopropylmethyl; R₂ = trifluoromethyl

8-21, 26-29, 31, 32, 34

^aReagents and conditions: (a) amine, 2-(2'-di-*tert*-butylphosphine)-biphenylpalladium(II) acetate, K₃PO₄, 1,4-dioxane, 85 °C, 2–12 h; (b) amine, DIPEA, CH₃CN, 140–170 °C, 10–35 min, microwave; (c) amine, Pd(OAc)₂, BINAP, ^tBuONa, toluene, 100 °C, 16 h.

intermediates **41a–g** and **46** with an array of commercially available amines either under palladium-catalyzed cross-coupling reaction or by nucleophilic substitution under microwave heating conditions afforded the target compounds **8–21**, **26–29**, **31**, **32**, and **34**, whose chemical structures are shown in Tables 1–3.

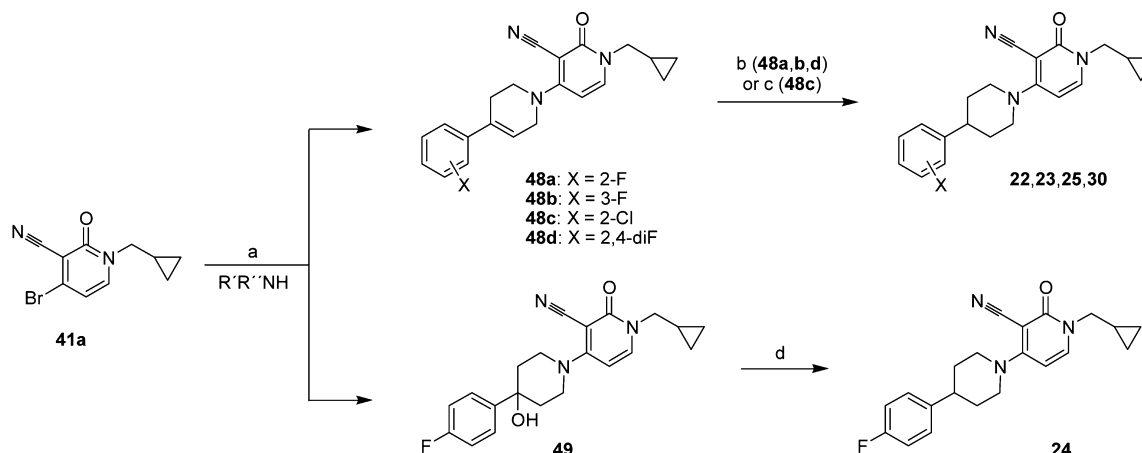
The 4-substituted-1-cyclopropylmethyl-3-cyano-2-pyridones **22–25** and **30** were prepared following the synthesis sequence shown in Scheme 3. Nucleophilic substitution of the 4-bromopyridone **41a** with the corresponding amines led to intermediates **48a–d** and **49**. Catalytic hydrogenation using Pd/C as the catalyst of compounds **48a–b** and **48d** yielded the target compounds **22**, **23**, and **30**. For intermediate **48c**, the hydrogenation reaction was accomplished by using PtO₂ as catalyst, yielding compound **25**. Treatment of intermediate **49** with triethylsilane in TFA led to the final compound **24**.

The synthesis of the 3-chloropyridone derivatives **33**, **35**, and **36** was achieved in two steps by Buchwald coupling reaction of the corresponding amines with intermediates **47a–c** followed by chlorination of the resulting pyridones **50a–c** with NCS in DCM (Scheme 4).

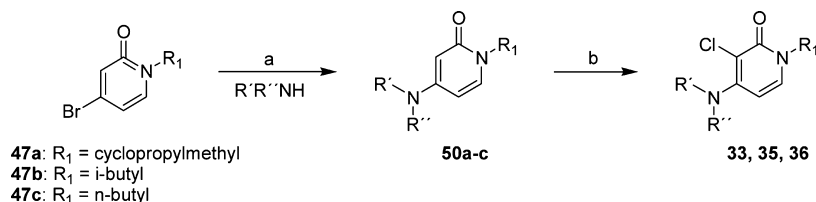
Finally, compounds **6** and **7** were prepared following the reaction pathway depicted in Scheme 5. Sonogashira coupling reaction of intermediate **41d** with phenylacetylene gave derivative **51**, which was converted into the target compound **6** by catalytic hydrogenation of the triple bond. Alkylation of **40d** with benzyl bromide under microwave irradiation afforded compound **7**.

RESULTS AND DISCUSSION

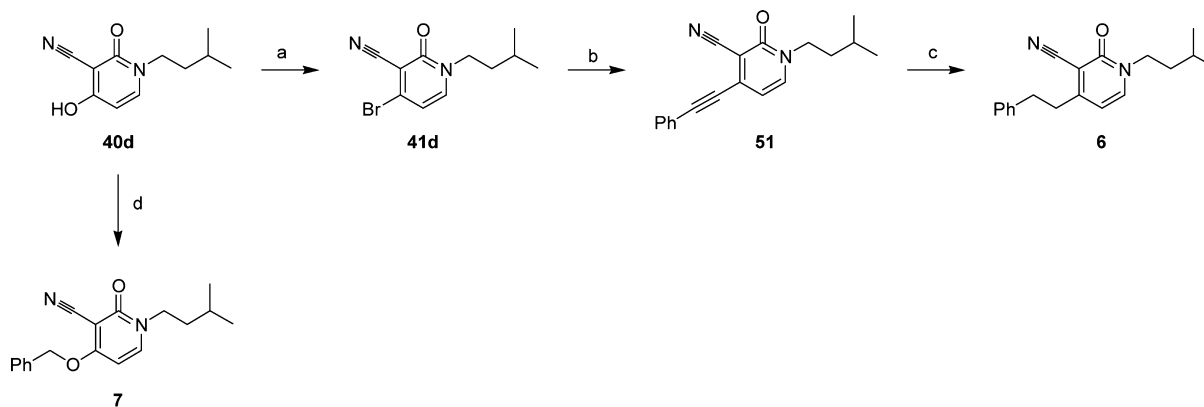
Guided by our previously reported overlay model for mGlu2 receptor PAM chemotypes,³⁰ we expanded the SAR around the 1,4-pyridone series by focusing on introducing a spacer (X)

Scheme 3. Synthesis of the Final Compounds 22–25 and 30^a

^aReagents and conditions: (a) amine, DIPEA, CH₃CN, 140–170 °C, 10–35 min, microwave; (b) H₂, Pd/C, MeOH or AcOEt, rt, 4–16 h; (c) H₂, PtO₂, AcOH, MeOH, rt, 72 h; (d) Et₃SiH, TFA, rt, 24 h.

Scheme 4. Synthesis of the Final Compounds 33, 35, and 36^a

^aReagents and conditions: (a) amine, Pd(OAc)₂, BINAP, ^tBuONa, toluene, 100 °C, 16 h; (b) NCS, DCM, rt, 10–20 min.

Scheme 5. Synthesis of the Final Compounds 6 and 7^a

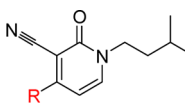
^aReagents and conditions: (a) POBr₃, DMF, 110 °C, 1–3 h; (b) phenylacetylene, PdCl₂(PPh₃)₂, Et₃N, CuI, PPh₃, THF, 90 °C, 10 h; (c) H₂, Pd/C, MeOH, rt, 3 h; (d) BnBr, Cs₂CO₃, CH₃CN/DMF, 130 °C, 20 min, microwave.

between the pyridone core and the phenyl ring (Figure 1). Representative compounds illustrating the new SAR generated along with mGlu2 receptor functional activity and metabolic stability data are shown in Table 1. Introduction of ethylene and methoxy linkers (**6** and **7**) led to a 13- and 3-fold increase in potency (EC₅₀⁴⁵), respectively, when compared to that of **5**. However, that improvement was not observed in compound **8** that has methylamino as the linker. Conformational restriction of compound **8** by means of cyclization of the nitrogen spacer onto the phenyl ring, as in isoquinoline derivative **9**, resulted in a remarkable 12-fold potency increase (**9**, EC₅₀ = 871 nM). Further modification around the isoquinoline group in **9** while keeping the piperidine fragment led to compounds **10** and **11**

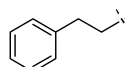
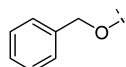
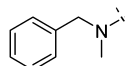
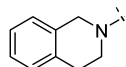
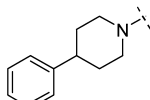
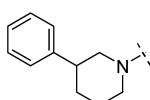
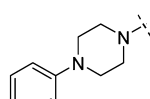
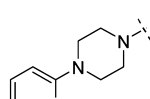
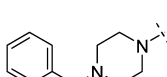
bearing a phenylpiperidine substituent. To our delight, the 4-phenylpiperidine derivative **10** exhibited a further boost in potency (EC₅₀ = 102 nM), whereas the regioisomer **11**, featuring 3-phenyl substitution on the piperidine, was markedly less active (EC₅₀ = 3311 nM).

The distal aromatic group in **10** seemed to be essential for achieving good activity, as the truncated analogue **12** showed barely measurable functional PAM activity of the mGlu2 receptor. Both findings suggest the importance of a lipophilic group linearly oriented by a spacer from the pyridone core. Replacement of the piperidine spacer by piperazine (**13**) led to a ~6-fold reduction in potency compared to that of the corresponding analogue **10**. Lastly, introducing a protonatable

Table 1. Functional Activity and Metabolic Stability Data of Representative mGlu2 Receptor PAMs 5–15



5-15

| Compd | R | mGluR2 EC ₅₀ (nM) ^a (95% CI) ^b | mGluR2 E _{MAX} (%) ^a ±SD | HLM (%) ^c | RLM (%) ^c |
|-------|---|--|--|----------------------|----------------------|
| 5 |  | 8,510 ^d | 135 ^d | 36 | 100 |
| 6 |  | 661 (487-876) | 168 ± 4 | 91 | 99 |
| 7 |  | 2,951 (2,726-3,122) | 173 ± 0 | 22 | 90 |
| 8 |  | 10,715 (3,467-33,113) | 249 ± 15 | 69 | 100 |
| 9 |  | 871 ^d | 310 ^d | 74 | 100 |
| 10 |  | 102 (84-128) | 26.8 ± 66 | 28 | 97 |
| 11 |  | 3,311 (2,414-4,542) | 231 ± 24 | 80 | 98 |
| 12 |  | 31,623 (30,227-33,083) | 185 ± 5 | 67 | 100 |
| 13 |  | 661 (487-876) | 118 ± 14 | 50 | 90 |
| 14 |  | 3,090 (2,824-3,382) | 304 ± 35 | 51 | 54 |
| 15 |  | 4,677 (2,601-8,410) | 304 ± 20 | 38 | 85 |

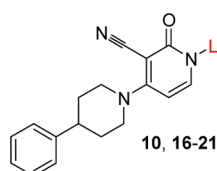
^aValues represent the mean for at least two experiments. ^bCI = confidence interval. ^cHLM and RLM data refer to the percent of compound metabolized after incubation with microsomes for 15 min at a 5 μM concentration. ^dCI and SD not determined.

partially basic nitrogen on the 4-phenylpiperazine template (**14** and **15**) was detrimental for the activity (EC₅₀ values of 3090 and 4677 nM respectively).

Alongside the assessment of activity, compounds **6–15** were assessed for in vitro P450-mediated oxidative stability in human and rat liver microsomes (HLM and RLM, respectively). The results shown in Table 1 indicate that most analogues suffered

from extensive metabolic degradation in RLM, with somewhat lower metabolic turnover in HLM. Interestingly analogue **10**, despite having high degradation in RLM (97% metabolized), was relatively stable in HLM (28% metabolized). Metabolic profiling studies on **10** suggested that the turnover in RLM could be attributed to oxidation of the *N*-isopentyl chain.⁴⁶

Table 2. Functional Activity, Metabolic Stability Data, and Calculated LogP of Representative 4-Phenylpiperidine-Substituted mGlu2 Receptor PAMs 10 and 16–21



| Compd | L | mGluR2 EC ₅₀ (nM) ^a (95% CI) ^b | mGluR2 E _{MAX} (%) ^a ±SD | HLM ^c (%) | RLM ^c (%) | cLogP ^d |
|-------|---|--|---|-------------------------|-------------------------|--------------------|
| 10 | | 102 (84-128) | 26.8 ± 6.6 | 28 | 97 | 4.17 |
| 16 | | 95 (78-115) | 309 ± 63 | 30 | 62 | 3.77 |
| 17 | | 282 (177-443) | 316 ± 47 | 37 | 47 | 3.64 |
| 18 | | 55 (48-62) | 269 ± 17 | 46 | 86 | 3.71 |
| 19 | | 151 (103-224) | 309 ± 56 | 25 | 44 | 3.16 |
| 20 | | 178 (155-204) | 316 ± 70 | 50 | 61 | 3.68 |
| 21 | | 355 (238-536) | 302 ± 45 | 18 | 43 | 3.28 |

^aValues represent the mean for at least two experiments. ^bCI = confidence interval. ^cHLM and RLM data refer to the percent of compound metabolized after 15 min at 5 μM concentration. ^dcLogP calculated with Biobyte software.

Given the notable increase in potency observed upon incorporation of the 4-phenylpiperidine substituent, we turned our attention to address the high metabolic turnover of **10** in RLM. The exploration began by focusing on replacing the isopentyl chain in **10** by alternative aliphatic groups that would decrease the overall lipophilicity of the molecule (see calculated LogP in Table 2, compounds **16–21**). As seen in Table 2, some isopentyl replacements (**17** and **19–21**) led to a slight decrease in activity. Some others, such as *n*-butyl (**16**), showed comparable potency, and cyclobutylmethyl (**18**) was the only replacement that showed superior potency (EC₅₀ = 55 nM) to that of **10**. Unfortunately, the metabolic stability in RLM of **18** did not improve significantly. Compound **19**, containing a cyclopropylmethyl chain and having the lowest lipophilicity (cLogP = 3.16), presented the best balance of potency and metabolism (EC₅₀ = 151 nM and HLM and RLM 25 and 44% metabolized, respectively). Detailed characterization of 3-cyano-1-cyclopropylmethyl-4-(4-phenylpiperidin-1-yl)-pyridine-2(1*H*)-one **19** (JNJ-40068782) has been recently published.⁴⁷

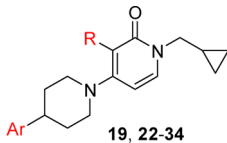
With the more optimal *N*-cyclopropylmethyl substituent identified, a sequential SAR expansion focusing first on the effect of substitution on the phenyl ring of **19** and second on alternative groups to the cyano substituent at the 3 position of the pyridone core was conducted. A representative set of analogues to exemplify the SAR trends identified is shown in Table 3. Overall, both electron-withdrawing and -donating substituents on the phenyl ring (**22–32**) were well-tolerated for potency, and the low metabolic turnover seen for **19** was retained for most examples. The *ortho* and *para* fluoro

substituent in compounds **22** and **24** led to a 2-fold potency increase, whereas the *meta* fluoro substituent (**23**) retained the activity observed with the nonsubstituted phenyl derivative **19**. When the fluorine atom in compounds **22** and **24** was replaced with the more lipophilic chlorine (**25** and **26**), an additional 2-fold increase in potency was obtained. The trifluoromethyl analogue **27** showed a consistent potency increase, with an EC₅₀ of 46 nM.

In the case of electron-donating substituents, such as methoxy, *ortho* substitution was preferred versus *para* substitution and thus compound **28** (EC₅₀ = 35 nM) was found to be ~3-fold more active than **29** (EC₅₀ = 180 nM). Unfortunately, methoxy-substituted compounds were prone to higher metabolic degradation in both HLM and RLM. Some additive effects were observed while mapping the phenyl ring with two fluorine substituents (**30–32**), with compound **31**, featuring the bis-*ortho* substitution, showing the better activity (EC₅₀ = 31 nM). Finally, SAR from previously reported series³¹ prompted us to study the effect of replacing the cyano group by chlorine and trifluoromethyl substituents. Relative to **19**, compound **33**, bearing a chlorine substituent, displayed slightly lower potency (EC₅₀ = 170 nM) and comparable metabolic stability. The trifluoromethyl-substituted analogue **34** was found to be ~2-fold less potent than **19** (EC₅₀ = 251 nM) and presented a pronounced metabolic turnover in RLM. In contrast to previous SAR trends,³² the increased lipophilicity of **33** and **34** relative to **19** did not result in more potent compounds.

A set of compounds (**19–24**, **26–28**, and **31–33**) was then investigated for their ability to inhibit the hERG channel in an

Table 3. Functional Activity, Metabolic Stability Data, Calculated LogP, and hERG Inhibition Data of Representative Set of Aryl Modified mGlu2 Receptor PAMs 19 and 22–34



19, 22-34

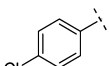
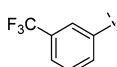
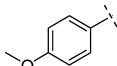
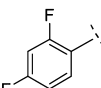
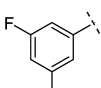
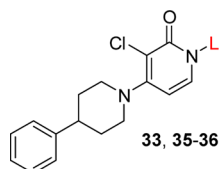
| Compd | Ar | R | mGluR2 EC ₅₀ (nM) ^a (95% CI) ^b | mGluR2 E _{MAX} (%) ^a ±SD | HLM ^c (%) | RLM ^c (%) | cLogP ^d | hERG ^e |
|-------|---|-----------------|--|---|-------------------------|-------------------------|--------------------|-------------------|
| 19 |  | CN | 151 (103-224) | 309 ± 56 | 25 | 44 | 3.16 | 58 |
| 22 |  | CN | 81 (71-93) | 282 ± 27 | 30 | 42 | 3.3 | 75 |
| 23 |  | CN | 141 (112-181) | 268 ± 39 | 35 | 37 | 3.3 | 87 |
| 24 |  | CN | 89 (55-141) | 258 ± 25 | 31 | 36 | 3.3 | 89 |
| 25 |  | CN | 49 (38-62) | 259 ± 36 | 22 | 34 | 3.87 | - |
| 26 |  | CN | 48 (29-79) | 249 ± 31 | 28 | 21 | 3.87 | 95 |
| 27 |  | CN | 46 (25-82) | 191 ± 7 | 35 | 39 | 4.04 | 97 |
| 28 |  | CN | 35 (27-45) | 265 ± 47 | 53 | 68 | 3.07 | 65 |
| 29 |  | CN | 98 (42-223) | 257 ± 28 | 76 | 57 | 3.07 | - |
| 30 |  | CN | 68 (47-100) | 272 ± 44 | 17 | 34 | 3.44 | -- |
| 31 |  | CN | 31 (18-52) | 291 ± 23 | 18 | 42 | 3.44 | 86 |
| 32 |  | CN | 151 (94-240) | 234 ± 13 | 30 | 45 | 3.44 | 95 |
| 33 |  | Cl | 170 (161-175) | 259 ± 38 | 17 | 30 | 4.25 | 51 |
| 34 |  | CF ₃ | 251 (166-379) | 239 ± 41 | 33 | 89 | 4.49 | - |

Table 3. continued

^aValues represent the mean for at least two experiments. ^bCI = confidence interval. ^cHLM and RLM data refer to the percent of compound metabolized after 15 min at 5 μ M concentration. ^dcLogP calculated with Biobyte software. ^eExperiments were performed using HEK293 cells stably transfected with the hERG potassium channel. Whole-cell currents were recorded with an automated patch-clamp system (PatchXpress 7000A). Three concentrations of compound were tested (0.1, 0.3, and 3 μ M; $n = 3$) and compared to vehicle (0.1% DMSO; $n = 3$). Data are presented as the percent inhibition at the highest concentration tested (3 μ M).

Table 4. Functional Activity, Metabolic Stability Data, Calculated LogP, and hERG Inhibition Data of Representative Set of Aryl-Modified mGlu2 Receptor PAMs 33, 35, and 36



| Compd | L | mGluR2 EC ₅₀ | mGluR2 | HLM ^c | RLM ^c | cLogP ^d | hERG ^e |
|-------|---|---|--|------------------|------------------|--------------------|-------------------|
| | | (nM) ^a (95% CI) ^b | E _{MAX} (%) ^a ± SD | (%) | (%) | | |
| 33 | | 170 (161-175) | 259 ± 38 | 17 | 30 | 4.25 | 51 |
| 35 | | 195 (155-245) | 260 ± 35 | 12 | 31 | 4.73 | 24 |
| 36 | | 147 (132-160) | 273 ± 32 | 23 | 53 | 4.86 | 43 |

^aValues represent the mean for at least two experiments. ^bCI = confidence interval. ^cHLM and RLM data refer to the percent of compound metabolized after 15 min at 5 μ M concentration. ^dcLogP calculated with Biobyte software. ^eExperiments were performed using HEK293 cells stably transfected with the hERG potassium channel. Whole-cell currents were recorded with an automated patch-clamp system (PatchXpress 7000A). Three concentrations of compound were tested (0.1, 0.3, and 3 μ M; $n = 3$) and compared to vehicle (0.1% DMSO; $n = 3$). Data are presented as the percent inhibition at the highest concentration tested (3 μ M).

Table 5. PK Data for Compounds 19, 33, 35, and 36 after Oral and i.v. Administration in Male Sprague–Dawley Rats^a and in Vivo Activity in the swEEG Model in Rats

| compd | Cl (mL, min ⁻¹ kg ⁻¹) ^b | T _{1/2} (h) ^b | T _{max} (h) ^b | AUC _{0–inf} (ng h/mL) ^b | C _{max} (ng/mL) ^b | F (%) | B/P ^c | swEEG ^d LAD/LAC |
|-------|---|-----------------------------------|-----------------------------------|---|---------------------------------------|-------|------------------|----------------------------|
| 19 | 18 ± 8.0 | 2.1 ± 0.1 | 0.5 ± 0.0 | 4350 ± 895 | 1407 ± 391 | 51 | 0.3 | 3/420 |
| 33 | 24 ± 4.0 | 3.5 ± 0.3 | 0.5 ± 0.0 | 2312 ± 516 | 986 ± 154 | 34 | 0.9 | >10/>986 |
| 35 | 13 ± 4.0 | 2.6 ± 0.5 | 0.7 ± 0.3 | 3455 ± 734 | 1357 ± 214 | 25 | 0.8 | 3/407 |
| 36 | 23 ± 1.0 | 2.3 ± 0.5 | 0.5 ± 0.0 | 2250 ± 417 | 938 ± 300 | 31 | 1 | 3/281 |

^aStudy in male Sprague–Dawley rats dosed at 10 mg/kg p.o. and 2.5 mg/kg iv, formulated in 20% HP- β -CD + HCl solution at pH 4. ^bValues are the mean of three animals ± SEM. ^cRatios calculated after 1 h of a single dose at 10 mg/kg sc in 1 mg/mL in 20% HP- β -CD + HCl solution at pH 4 in the Swiss mouse. ^dCompound given orally. LAD stands for lowest active dose expressed in mg/kg. LAC stands for lowest active concentration in plasma, at active doses estimated on the basis of C_{max} expressed in ng/mL.

electrophysiology patch-clamp study. The inhibition of the hERG channel is an indicator for potential QTc prolongation and potential for serious cardiac arrhythmias. Unfortunately, most of the compounds inhibited the hERG channel in >55% at the highest concentration tested (3 μ M). Thus, in the case of 3-cyanopyridones, the more lipophilic molecules (26, 27, and 32) showed higher hERG inhibitory activity. Interestingly, despite its high lipophilicity (cLogP = 4.25), the 3-chloropyridone derivative 33 exhibited the lowest hERG inhibition value (51%). However, more detailed in vivo cardiovascular safety studies are required to put the hERG inhibition data into a meaningful context. On the basis of the described profile, compounds 18 and 33 were progressed to in vivo pharmacokinetics studies to further understand the potential of the series.

Thus, 19 and 33 were assessed for their ability to cross the blood–brain barrier (BBB) after a subcutaneous dose of 10 mg/kg in mice. As shown in Table 5, compound 33 displayed a higher brain-to-plasma (B/P) ratio of 0.9 vs 0.3 for 19. Given the requirement for adequate BBB penetration, further exploration of 3-cyanopyridones was halted while we instead sought to fine tune the hERG interaction of the 3-chloropyridone lead 33. Two compounds with different alkyl chains attached to the pyridone nitrogen were synthesized (35 and 36), and their data are shown in Table 4. Thus, compounds 35 and 36, having an iso-butyl or butyl chain, respectively, showed comparable potency (35: EC₅₀ = 195 nM and 36: EC₅₀ = 147 nM) and metabolic stability to that of 33. More interestingly, both compounds had reduced hERG inhibition (35: 24%; 36: 43% at 3 μ M).

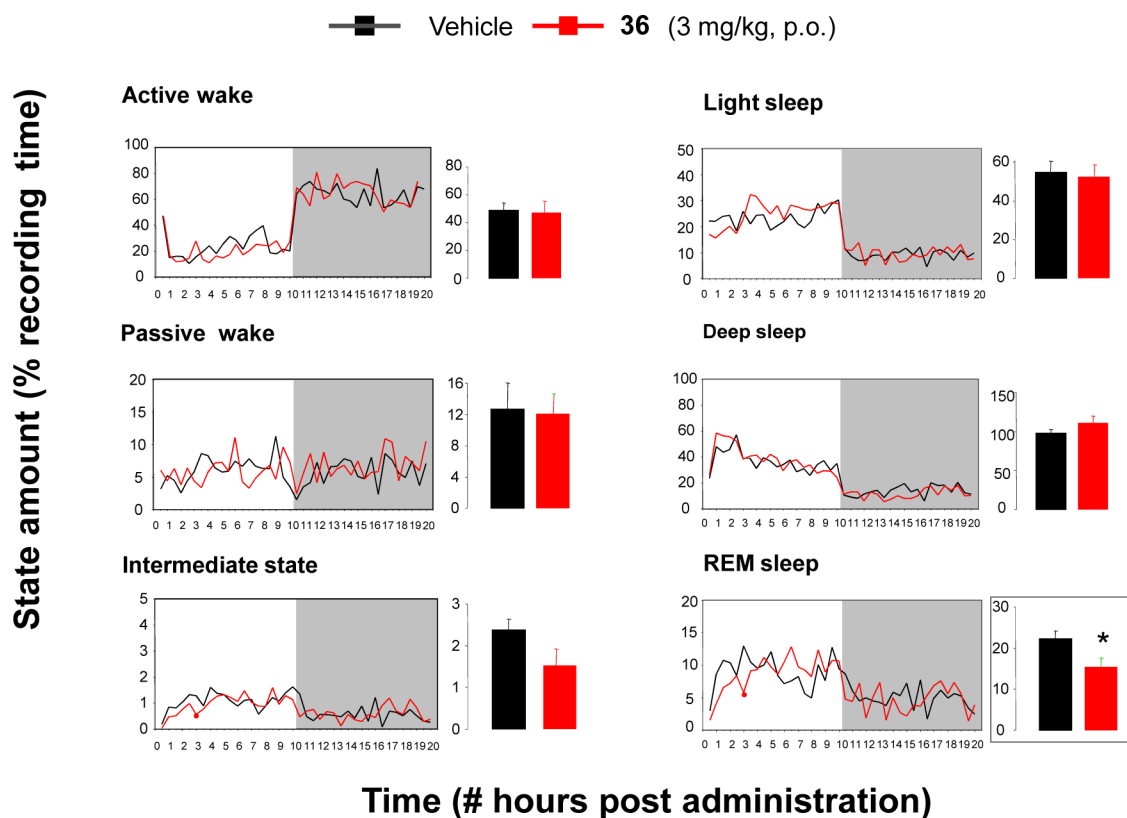


Figure 2. Effect of 36 or vehicle (20% CD + 1HCl) on sleep–wake organization in rats during 20 consecutive hours and after a single oral dose. Mean percentage of occurrence per 30 min period is indicated for each sleep–wake state. Shaded area indicates dark period. Small bar charts indicate amounts of vigilance states in minutes (\pm SEM, $n = 8$ for each group) during the first 4 h postadministration. Dots on the lines of the graph indicate $p < 0.05$ versus vehicle (Wilcoxon–Mann–Whitney rank sum); * indicates $p < 0.05$: Wilcoxon–Mann–Whitney rank sum tests compared to vehicle values.

Because of their overall favorable attributes, compounds 35 and 36 along with 19 and 33 were investigated further to ascertain their drug-like properties as well as in vivo activity. Overall, the four compounds exhibited relatively comparable rat PK data (Table 5). After intravenous (i.v.) administration, all compounds presented low-to-moderate plasma clearance (Cl), with compounds 33 and 36 having higher values. When dosed orally (p.o.), plasma concentrations declined in comparable magnitude for all of the compounds with relatively short half-lives ($T_{1/2}$ between 2.1 and 3.5 h). The mean maximum plasma concentrations (C_{max}) were reached at 0.5–0.7 h postdose and were in the range of ~900 to ~1400 ng h/mL, indicating a fast absorption rate. Plasma exposure (AUC_{0-inf}) was relatively good for all compounds, ranging between ~2000 and ~4350 ng h/mL, and this resulted in moderate absolute oral bioavailabilities (F %) between 25 and 51%. As expected, B/P ratios observed of compounds 35 and 36 were comparable to that of compound 33, previously discussed.

As in previously reported series, the in vivo pharmacological activity of the compounds was investigated in the sleep–wake EEG (swEEG) paradigm.^{29,31,32} It has been previously shown that selective activation or positive allosteric modulation of the mGlu2 receptor in vivo affects the sleep–wake architecture in rats and mice.^{48,49} After acute p.o. administration of a 3 mg/kg dose, compounds 19, 35, and 36, but not 33, significantly decreased the amount of REM sleep in rats during the first 4 h without clear effects on the other sleep–wake stages (see 36 in Figure 2, bottom right panel, as a representative example). The active dose of 3 mg/kg p.o. corresponded to plasma

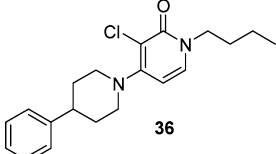
concentrations of ~420, 407, and 281 ng/mL for compounds 19, 35, and 36, respectively.

Compound 36 showed the best overall in vitro and in vivo profile among all of the analogues prepared, which prompted us to select it for an extensive characterization. A general profile of 36 is presented in Table 6. Compound 36 did not have significant activity against other mGlu receptor subtypes⁵⁰ with ≥ 30 -fold selectivity, exhibiting also ≥ 100 -fold selectivity versus a panel of diverse targets⁵¹ with only mild antagonist effect for the 5HT_{2A} receptor ($K_b = 1.1 \mu\text{M}$). Further characterization of the 5HT_{2A} interaction will be described in more detail in a separate publication.

Radioligand binding studies were performed using [³H]19 as an allosteric mGlu2 receptor radioligand⁴⁷ and confirmed that 36 binds to an allosteric site with high affinity ($IC_{50} = 68 \text{ nM}$)

Compound 36 showed low aqueous solubility (<0.001 mg/mL), which was not influenced by the pH; nevertheless, the solubility of 36 increased in complexation with cyclodextrins and thus with 20% HP- β -CD it reached 2.20 mg/mL at pH 4.16. Caco-2 data showed high permeability with no indication for an efflux mechanism such as P-gp. Elimination half-lives were moderate across different species. Volume of distribution across species was equal to or a little higher than total body water (0.8–1.8 L/kg), indicative of compound distribution outside of the plasma. Oral bioavailability was low to moderate across mouse, rat, dog and monkey (6–31%). The predicted in vitro hepatic clearance for the rat, dog, monkey, and human suggested that phase 1 metabolism via the CYP450 enzymes contributes largely to the in vivo plasma clearance of the

Table 6. Overview of 36



| | |
|---------------------------------------|---|
| physicochemical properties | MW = 344 |
| | Experimental $pK_a < 2$ |
| | Experimental $\log P = 4.6$ at pH 6.8 |
| in vitro pharmacology | mGlu2 PAM $EC_{50} = 147 \pm 42$ nM; $E_{max} = 273 \pm 32\%$ |
| | mGlu2 PAM binding $IC_{50} \sim 68 \pm 29$ nM |
| | Selectivity (mGlu 1.3–8; CEREP) ≥ 30 -fold vs mGlu2 PAM but $5HT_{2A}$ (~ 10 -fold) |
| ADME profile | Solubility < 0.001 mg/mL in water and 2.2 mg/mL 20% HP- β -CD at pH 4 |
| | Plasma Protein Binding (%) = 99.5 (h), 99.6 (r), 99.2 (ms), 99.4 (dog) |
| | Permeability (Caco-2 monolayers): High (AB/BA $P_{app} \times 10$ cm $s^{-1} = 12/6$) |
| | CYP450 inh. = 1A2, 2D6, 3A4 (> 18 μM), 2C9 (6 μM), 2C19 (7 μM) |
| rat PK: 2.5 mg/kg i.v.; 10 mg/kg p.o. | Cl = 23 mL/min/kg; $V_{dss} = 2.3$ L/kg; $T_{max} = 0.5$ h; $T_{1/2} = 2.3$ h |
| | AUC $_{0-inf} = 2250$ ng h/mL; $C_{max} = 938$ ng/mL; F (%) = 31; B/P ratio = 1 |
| dog PK: 1 mg/kg i.v.; 2.5 mg/kg p.o. | Cl = 23 mL/min/kg; $V_{dss} = 1.8$ L/kg; $T_{max} = 0.5$ h; $T_{1/2} = 3.7$ h |
| | AUC $_{0-inf} = 743$ ng.h/mL; $C_{max} = 373$ ng/mL; F (%) = 20 |
| swEEG rat p.o. | LAD = 3 mg/kg (free plasma conc. ~ 0.9 ng/mL) |
| CV safety | hERG PC ^a ; rabbit Purkinje fiber; anesthetized guinea-pig, and anesthetized dog; all margin $\geq 38^b$ |
| genotoxicity | Ames TA98 ^c : clean up to 125 mg/mL In vitro Micronucleus ^d : clean up to 150 $\mu g/mL$ |

^aExperiments were performed using HEK293 cells stably transfected with the hERG potassium channel. Whole-cell currents were recorded with an automated patch-clamp system (PatchXpress7000A). Three concentrations of compound were tested (0.1, 0.3, and 3 μM ; $n = 3$) and compared with vehicle (0.1% DMSO; $n = 3$). Data are presented as the percent inhibition at the highest concentration tested (3 μM). ^bBased on efficacy free concentration in sw-EEG model (~ 0.9 ng/mL). ^cIn vitro bacterial reverse mutation assay in *Salmonella typhimurium* TA98. ^dStudy conducted in human lymphoblastoid TK6 cell line in the presence or absence of metabolic activation (rat liver S9).

compound. The calculated hepatic clearance corresponded to ~ 45 – 55% of the hepatic blood flow across the species. Compound 36 does not inhibit CYP450 enzymes significantly and is predominantly metabolized by CYP 3A4. Plasma protein binding was consistently high across the species. Compound 36 showed good safety margins in various cardiovascular studies and no indication of genotoxicity or cytotoxicity.

CONCLUSIONS

Further optimization of the 1,4-disubstituted cyanopyridone series of mGlu2 receptor PAMs was performed. Strategic exploration of the SAR led to a novel generation of pyridones with a more optimal balance between potency, PK, and CV safety. Our lead optimization efforts have led to the discovery of 36 as a potent, selective mGlu2 receptor PAM, which is orally bioavailable and safe. In an exploratory phase 2a study in schizophrenia, not powered to determine statistical significance

of effects but rather used as a signal generation study, 36 met the primary objectives of safety and tolerability and also demonstrated an effect in patients with residual negative symptoms. Further evaluation of this signal in a formal proof-of-concept study is warranted in patients with residual negative symptoms. In contrast, in patients with MDD with significant anxiety symptoms, 36 failed to meet the criterion for efficacy signal. Despite this lack of signal on the primary outcome measure, treatment with 36 showed mixed and modest efficacy signals on several anxiety measures and on all depression measures.

The data collected from the clinical trials with 36 undoubtedly provides valuable information and should help to better assess the potential of the mGlu2 receptor as a viable target for the treatment of CNS disorders. To that end, finding the right patient population that may be benefit from treatment with an mGlu2 modulator is still a challenge that must be addressed.

EXPERIMENTAL SECTION

Chemistry. Unless otherwise noted, all reagents and solvents were obtained from commercial suppliers and used without further purification. Synthesis of intermediates 39a,c,d,e, 40a,c,d,e, and 41a,c,d,e and final compound 5 were previously described.²⁸ Thin-layer chromatography (TLC) was carried out on silica gel 60 F254 plates (Merck). Flash column chromatography was performed on silica gel (particle size 60 Å, mesh = 230–400 (Merck)) using standard techniques. Microwave-assisted reactions were performed in a single-mode reactor, Biotage Initiator Sixty microwave reactor (Biotage), or in a multimode reactor, MicroSYNTH Labstation (Milestone, Inc.). Nuclear magnetic resonance (NMR) spectra were recorded with either a Bruker DPX-400 or a Bruker AV-500 spectrometer (broaduker AG) with standard pulse sequences, operating at 400 and 500 MHz, respectively, using $CDCl_3$ and $DMSO-d_6$ as solvents. Chemical shifts (δ) are reported in parts per million (ppm) downfield from tetramethylsilane ($\delta = 0$). Coupling constants are reported in Hertz. Splitting patterns are defined by s (singlet), d (doublet), dd (double doublet), t (triplet), q (quartet), quin (quintet), sex (sextet), sep (septet), or m (multiplet). Liquid chromatography combined with mass spectrometry (LC–MS) was performed on a HP 1100 HPLC system (Agilent Technologies) comprising a quaternary or binary pump with degasser, an autosampler, a column oven, a diode-array detector (DAD), and a column. Flow from the column was split to a MS spectrometer. The MS detector was configured either with an electrospray ionization source or an ESCI dual ionization source (electrospray combined with atmospheric pressure chemical ionization). Nitrogen was used as the nebulizer gas. Data acquisition was performed with MassLynx-Openlynx software or with Chemstation-Agilent Data Browser software. Gas chromatography combined with mass spectrometry (GC–MS) was performed using a 6890 series gas chromatograph (Agilent Technologies) system comprising a 7683 series injector and autosampler, a column oven, and a J&W HP-5MS coupled to a 5973N MSD mass selective detector (single quadrupole, Agilent Technologies). The MS detector was configured with an electronic impact ionization source/chemical ionization source (EI/CI). EI low-resolution mass spectra were acquired by scanning from 50 to 550 at a rate of 14.29 scans/s. The source temperature was maintained at 230 °C. Helium was used as the nebulizer gas. Data acquisition was performed with Chemstation-Open Action software. Melting point (mp) values are peak values obtained with experimental uncertainties that are commonly associated with this analytical method and were determined in open capillary tubes on a Mettler FP62 apparatus with a temperature gradient of 10 °C/min. Maximum temperature was 300 °C.

Purities of all new compounds were determined by analytical reverse-phase RP-HPLC using the area percentage method on the UV

trace recorded at a wavelength of 254 nm and were found to have $\geq 95\%$ purity, unless otherwise specified.

1-Isopentyl-2-oxo-4-phenethyl-1,2-dihydropyridine-3-carbonitrile (6). A mixture of 1-isopentyl-2-oxo-4-(2-phenylethynyl)-1,2-dihydropyridine-3-carbonitrile **39d** (45 mg, 0.2 mmol) and 10% Pd/C (0.01 g, catalyst) in MeOH (5 mL) was hydrogenated for 3 h at room temperature. The catalyst was filtered off under nitrogen atmosphere, and the filtrate solvent was evaporated. The crude was purified by flash column chromatography (silica gel, MeOH in CH_2Cl_2 , 0:100 to 4:96). Desired fractions were collected, and the solvent was evaporated. The residue was further purified by preparative reverse phase HPLC (C18 XSelect 19 \times 100 mm 5 μm , 20–100% $\text{CH}_3\text{CN}/0.1\% \text{NH}_4\text{CO}_3\text{H}/\text{NH}_4\text{OH}$ pH 9 solution in water) to yield **6** (1.6 mg, 4%). ^1H NMR (500 MHz, CDCl_3) δ 0.96 (d, $J = 6.4$ Hz, 6H), 1.58–1.65 (m, 3H), 2.92–3.04 (m, 4H), 3.92–3.97 (m, 2H), 6.04 (d, $J = 6.9$ Hz, 1H), 7.16–7.24 (m, 3H), 7.27–7.32 (m, 2H), 7.35 (d, $J = 6.9$ Hz, 1H). LC–MS m/z 295 $[\text{M} + \text{H}]^+$.

4-Benzylloxy-1-isopentyl-2-oxo-1,2-dihydropyridine-3-carbonitrile (7). Benzyl bromide (88.2 μL , 0.7 mmol) was added to a mixture of **40d** (102 mg, 0.5 mmol) and CsCO_3 (319 mg, 1 mmol) in CH_3CN (2 mL) and DMF (1 mL). The reaction mixture was heated in a microwave oven at 130 $^\circ\text{C}$ for 20 min. The solid was filtered off through a Celite pad and washed with EtOAc (10 mL). The combined organic filtrates were evaporated in vacuo, and the residue was purified by flash column chromatography (silica gel, silica gel, MeOH in CH_2Cl_2 , 0:100 to 4:96). Desired fractions were collected, and the solvent was evaporated to yield compound **7** as a white solid (115 mg, 79%). mp 173.8 $^\circ\text{C}$. ^1H NMR (400 MHz, CDCl_3) δ 0.95 (d, $J = 5.8$ Hz, 6H), 1.54–1.67 (m, 3H), 3.88–3.94 (m, 2H), 5.28 (s, 2H), 6.06 (d, $J = 7.7$ Hz, 1H), 7.31–7.45 (m, 6H). LC–MS m/z 297 $[\text{M} + \text{H}]^+$.

4-Benzyl(methyl)aminol-1-isopentyl-2-oxo-1,2-dihydropyridine-3-carbonitrile (8). A mixture of **41d** (50 mg, 0.2 mmol), *N*-methylbenzylamine (28.8 mg, 0.2 mmol), 2-(2'-di-*tert*-butylphosphine)biphenylpalladium(II) acetate (4.6 mg, 0.01 mmol), K_3PO_4 (90 mg, 0.4 mmol), and 1,4-dioxane (6 mL) was heated at 85 $^\circ\text{C}$ for 6 h. The mixture was cooled to room temperature and filtered through a Celite pad. The solid was washed with more 1,4-dioxane (10 mL). The organic filtrate was evaporated, and the residue was purified by flash column chromatography (silica gel, silica gel, MeOH– NH_3 in CH_2Cl_2 , 0:100 to 4:96). Desired fractions were collected, and the solvent was evaporated to yield compound **8** (39 mg, 66%). ^1H NMR (400 MHz, CDCl_3) δ 0.94 (d, $J = 6.2$ Hz, 6H), 1.53–1.67 (m, 3H), 3.35 (s, 3H), 3.79–3.86 (m, 2H), 4.73 (s, 2H), 5.77 (d, $J = 8.1$ Hz, 1H), 7.10 (d, $J = 8.1$ Hz, 1H), 7.15–7.20 (m, 2H), 7.28–7.34 (m, 1H), 7.34–7.41 (m, 2H). LC–MS m/z 310 $[\text{M} + \text{H}]^+$.

4-(3,4-Dihydro-1H-isoquinolin-2-yl)-1-isopentyl-2-oxo-1,2-dihydropyridine-3-carbonitrile (9). Starting from **41d** (120 mg, 0.4 mmol) and 1,2,3,4-tetrahydroisoquinoline following the procedure described for **8**, compound **9** was obtained as a white solid (78 mg, 54%). mp > 300. ^1H NMR (400 MHz, CDCl_3) δ 0.95 (d, $J = 6.4$ Hz, 6H), 1.53–1.66 (m, 3H), 3.05 (t, $J = 5.9$ Hz, 2H), 3.82–3.88 (m, 2H), 3.91 (t, $J = 5.9$ Hz, 2H), 4.78 (s, 2H), 5.92 (d, $J = 8.1$ Hz, 1H), 7.12–7.26 (m, 5H). LC–MS m/z 322 $[\text{M} + \text{H}]^+$.

1-Isopentyl-2-oxo-4-(4-phenyl-1-piperidyl)-1,2-dihydropyridine-3-carbonitrile (10). DIPEA (0.233 mL, 1.34 mmol) was added to a mixture of **41d** (300 mg, 1.12 mmol) and 4-phenylpiperidine (198 mg, 1.23 mmol) in CH_3CN (3 mL). The reaction mixture was heated at 150 $^\circ\text{C}$ for 10 min in a microwave oven. The solvent was evaporated, and the residue was purified by flash column chromatography (silica gel, silica gel, EtOAc in CH_2Cl_2 , 0:100 to 20:80). Desired fractions were collected, and the solvent was evaporated to yield compound **10** (296 mg, 63%) as a colorless oil that solidified upon standing. mp > 300. ^1H NMR (400 MHz, CDCl_3) δ 0.96 (d, $J = 6.2$ Hz, 6H), 1.54–1.68 (m, 3H), 1.84 (qd, $J = 12.5$, 3.9 Hz, 2H), 1.97–2.05 (m, 2H), 2.82 (tt, $J = 12.1$, 3.8 Hz, 1H), 3.18–3.27 (m, 2H), 3.82–3.89 (m, 2H), 4.27–4.35 (m, 2H), 5.89 (d, $J = 7.9$ Hz, 1H), 7.18 (d, $J = 7.9$ Hz, 1H), 7.20–7.26 (m, 3H), 7.29–7.36 (m, 2H). LC–MS m/z 350 $[\text{M} + \text{H}]^+$.

Isopentyl-2-oxo-4-(3-phenyl-1-piperidyl)pyridine-3-carbonitrile (11). Starting from **41d** (60 mg, 0.22 mmol) and 3-

phenylpiperidine (42.5 mg, 0.26 mmol) and following the procedure described for **8**, compound **11** was obtained as a white gummy solid (13 mg, 30%). ^1H NMR (400 MHz, CDCl_3) δ 0.95 (d, $J = 6.4$ Hz, 6H), 1.53–1.67 (m, 3H), 1.76–1.88 (m, 2H), 1.90–2.01 (m, 1H), 2.06–2.17 (m, 1H), 2.91 (tt, $J = 11.4$, 3.7 Hz, 1H), 3.03–3.18 (m, 2H), 3.80–3.87 (m, 2H), 4.12–4.21 (m, 1H), 4.24–4.33 (m, 1H), 5.85 (d, $J = 7.9$ Hz, 1H), 7.15 (d, $J = 7.9$ Hz, 1H), 7.22–7.37 (m, 5H). LC–MS m/z 350 $[\text{M} + \text{H}]^+$.

Isopentyl-2-oxo-4-(1-piperidyl)pyridine-3-carbonitrile (12). Starting from **41d** (110 mg, 0.60 mmol) and piperidine hydrobromide (119.5 mg, 0.72 mmol) and following the procedure described for **8**, compound **12** was obtained as a white solid (125 mg, 82%). mp 75.9 $^\circ\text{C}$. ^1H NMR (500 MHz, CDCl_3) δ 0.94 (d, $J = 6.4$ Hz, 6H), 1.53–1.66 (m, 3H), 1.71 (br s, 6H), 3.58–3.67 (m, 4H), 3.81–3.87 (m, 2H), 5.92 (d, $J = 7.8$ Hz, 1H), 7.25 (d, $J = 7.8$ Hz, 1H). LC–MS m/z 274 $[\text{M} + \text{H}]^+$.

Isopentyl-2-oxo-4-(4-phenylpiperazin-1-yl)pyridine-3-carbonitrile (13). Starting from **41d** (120 mg, 0.40 mmol) and 1-phenylpiperazine (77.87 mg, 0.48 mmol) and following the procedure described for **8**, compound **13** was obtained as a white solid (155 mg, 99%). mp > 300 $^\circ\text{C}$. ^1H NMR (400 MHz, CDCl_3) δ 0.95 (d, $J = 6.0$ Hz, 6H), 1.54–1.67 (m, 3H), 3.29–3.37 (m, 4H), 3.79–3.90 (m, 6H), 5.92 (d, $J = 7.9$ Hz, 1H), 6.87–6.96 (m, 3H), 7.23–7.32 (m, 3H). LC–MS m/z 351 $[\text{M} + \text{H}]^+$.

Isopentyl-2-oxo-4-[4-(2-pyridyl)piperazin-1-yl]pyridine-3-carbonitrile (14). Starting from **41d** (50 mg, 0.20 mmol) and 1-(2-pyridyl)piperazine (40.8 μL , 0.24 mmol) and following the procedure described for **8**, compound **14** was obtained as a white solid (60 mg, 95%). ^1H NMR (400 MHz, CDCl_3) δ 0.95 (d, $J = 6.2$ Hz, 6H), 1.54–1.69 (m, 3H), 3.71–3.77 (m, 4H), 3.81–3.89 (m, 6H), 5.91 (d, $J = 7.9$ Hz, 1H), 6.64 (d, $J = 8.5$ Hz, 1H), 6.68 (ddd, $J = 7.2$, 4.9, 0.7 Hz, 1H), 7.25 (d, $J = 7.9$ Hz, 1H), 7.53 (ddd, $J = 8.7$, 7.0, 2.1 Hz, 1H), 8.20 (ddd, $J = 5.0$, 1.9, 0.8 Hz, 1H). LC–MS m/z 352 $[\text{M} + \text{H}]^+$.

Isopentyl-2-oxo-4-(4-benzylpiperazin-1-yl)pyridine-3-carbonitrile (15). Starting from **41d** (120 mg, 0.40 mmol) and 1-benzylpiperazine (84.60 mg, 0.48 mmol) and following the procedure described for **8**, compound **15** was obtained as a white solid (150 mg, 93%). mp 131.6 $^\circ\text{C}$. ^1H NMR (400 MHz, CDCl_3) δ 0.94 (d, $J = 6.2$ Hz, 6H), 1.52–1.66 (m, 3H), 2.53–2.60 (m, 4H), 3.54 (s, 2H), 3.63–3.69 (m, 4H), 3.80–3.86 (m, 2H), 5.85 (d, $J = 7.9$ Hz, 1H), 7.21 (d, $J = 7.9$ Hz, 1H), 7.23–7.40 (m, 5H). LC–MS m/z 365 $[\text{M} + \text{H}]^+$.

Butyl-2-oxo-4-(4-phenyl-1-piperidyl)pyridine-3-carbonitrile (16). Starting from **41c** (1000 mg, 3.92 mmol) and 4-phenylpiperidine (821.6 mg, 5.09 mmol) and following the procedure described for **10**, compound **16** was obtained as a cream solid (1.24 g, 94%). mp 138.2 $^\circ\text{C}$. ^1H NMR (500 MHz, CDCl_3) δ 0.95 (t, $J = 7.4$ Hz, 3H), 1.36 (sxt, $J = 7.5$ Hz, 2H), 1.69 (quin, $J = 7.5$ Hz, 2H), 1.85 (qd, $J = 12.7$, 3.3 Hz, 2H), 1.97–2.05 (m, 2H), 2.82 (tt, $J = 12.1$, 3.5 Hz, 1H), 3.23 (br t, $J = 12.7$ Hz, 2H), 3.84 (t, $J = 7.4$ Hz, 2H), 4.28–4.35 (m, 2H), 5.87 (d, $J = 8.1$ Hz, 1H), 7.16 (d, $J = 7.8$ Hz, 1H), 7.19–7.25 (m, 3H), 7.29–7.35 (m, 2H). LC–MS m/z 336 $[\text{M} + \text{H}]^+$.

Isobutyl-2-oxo-4-(4-phenyl-1-piperidyl)pyridine-3-carbonitrile (17). Starting from **41b** (510 mg, 2.0 mmol) and 4-phenylpiperidine (386.9 mg, 2.4 mmol) and following the procedure described for **10**, compound **17** was obtained as a white solid (606 mg, 94%). ^1H NMR (500 MHz, CDCl_3) δ 0.94 (d, $J = 6.6$ Hz, 6H), 1.86 (qd, $J = 12.7$, 3.6 Hz, 2H), 1.98–2.06 (m, 2H), 2.15 (dq, $J = 13.7$, 6.8 Hz, 1H), 2.82 (tt, $J = 12.0$, 3.6 Hz, 1H), 3.19–3.28 (m, 2H), 3.65 (d, $J = 7.5$ Hz, 2H), 4.29–4.36 (m, 2H), 5.87 (d, $J = 8.1$ Hz, 1H), 7.13 (d, $J = 7.8$ Hz, 1H), 7.20–7.26 (m, 3H), 7.29–7.36 (m, 2H). LC–MS m/z 336 $[\text{M} + \text{H}]^+$.

1-(Cyclobutylmethyl)-2-oxo-4-(4-phenyl-1-piperidyl)pyridine-3-carbonitrile (18). Starting from **41e** (600 mg, 2.24 mmol) and 4-phenylpiperidine (435 mg, 2.69 mmol) and following the procedure described for **10**, compound **18** was obtained as a cream solid (749.4 mg, 96%). mp 158.1 $^\circ\text{C}$. ^1H NMR (400 MHz, $\text{DMSO}-d_6$) δ 1.62–1.98 (m, 10H), 2.63 (quin, $J = 7.7$ Hz, 1H), 2.86 (tt, $J = 12.1$, 3.5 Hz, 1H), 3.17–3.27 (m, 2H), 3.81 (d, $J = 7.4$ Hz, 2H), 4.21–4.29 (m, 2H), 6.16 (d, $J = 8.1$ Hz, 1H), 7.18–7.23 (m, 1H), 7.24–7.34 (m, 5H). LC–MS m/z 348 $[\text{M} + \text{H}]^+$.

1-(Cyclopropylmethyl)-2-oxo-4-(4-phenyl-1-piperidyl)-pyridine-3-carbonitrile (19). Starting from **41a** (0.3 g, 1.18 mmol) and following the procedure described for **10**, compound **19** was obtained as a solid (285 mg, 73%). mp 128.4. ¹H NMR (500 MHz, CDCl₃) δ 0.31–0.42 (m, 2H), 0.55–0.66 (m, 2H), 1.15–1.24 (m, 1H), 1.85 (qd, *J* = 12.7, 3.8 Hz, 2H), 1.97–2.05 (m, 2H), 2.82 (tt, *J* = 12.1, 3.8 Hz, 1H), 3.19–3.28 (m, 2H), 3.71 (d, *J* = 7.2 Hz, 2H), 4.28–4.37 (m, 2H), 5.90 (d, *J* = 7.8 Hz, 1H), 7.20–7.26 (m, 3H), 7.28–7.36 (m, 3H). LC–MS *m/z* 334 [M + H]⁺.

1-(2-Cyclopropylethyl)-2-oxo-4-(4-phenyl-1-piperidyl)-pyridine-3-carbonitrile (20). Starting from **41f** (0.2 g, 0.748 mmol) and following the procedure described for **10**, compound **20** was obtained as a solid (200 mg, 77%). mp > 300. ¹H NMR (500 MHz, CDCl₃) δ 0.03–0.10 (m, 2H), 0.40–0.52 (m, 2H), 0.59–0.69 (m, 1H), 1.57–1.66 (m, 2H), 1.79–1.90 (m, 2H), 1.97–2.05 (m, 2H), 2.77–2.86 (m, 1H), 3.23 (br t, *J* = 12.9 Hz, 2H), 3.92 (br t, *J* = 6.8 Hz, 2H), 4.32 (br d, *J* = 13.3 Hz, 2H), 5.86 (d, *J* = 8.1 Hz, 1H), 7.18–7.26 (m, 4H), 7.29–7.36 (m, 2H). LC–MS *m/z* 348 [M + H]⁺.

2-Oxo-4-(4-phenyl-1-piperidyl)-1-(4,4,4-trifluorobutyl)-pyridine-3-carbonitrile (21). Starting from **41g** (0.25 g, 0.81 mmol) and following the procedure described for **10**, compound **21** was obtained as a solid (300 mg, 95%). mp 113.2 °C. ¹H NMR (500 MHz, CDCl₃) δ 1.78 (qd, *J* = 12.7, 3.8 Hz, 2H), 1.89–2.02 (m, 4H), 2.04–2.16 (m, 2H), 2.77 (tt, *J* = 12.1, 3.6 Hz, 1H), 3.14–3.23 (m, 2H), 3.85 (br t, *J* = 7.1 Hz, 2H), 4.27 (br d, *J* = 13.3 Hz, 2H), 5.85 (d, *J* = 8.1 Hz, 1H), 7.07 (d, *J* = 7.8 Hz, 1H), 7.12–7.21 (m, 3H), 7.22–7.29 (m, 2H). LC–MS *m/z* 390 [M + H]⁺.

1-(Cyclopropylmethyl)-4-[4-(2-fluorophenyl)-1-piperidyl]-2-oxo-pyridine-3-carbonitrile (22). A solution of **48a** (0.185 g, 0.52 mmol) in EtOAc (15 mL) was hydrogenated (atmospheric pressure) with Pd/C (37 mg) as a catalyst at room temperature for 4 h. The mixture was filtered through a Celite pad, and the filtrate was evaporated in vacuo. The crude was purified by flash column chromatography (silica gel, MeOH–NH₃ in CH₂Cl₂, 0:100 to 2:98) to give **22** as a pale yellow solid (148.3 mg, 80%). ¹H NMR (400 MHz, CDCl₃) δ 0.31–0.44 (m, 2H), 0.55–0.68 (m, 2H), 1.16–1.25 (m, 1H), 1.88 (qd, *J* = 12.4, 3.7 Hz, 2H), 1.97–2.05 (m, 2H), 3.18 (tt, *J* = 12.0, 3.9 Hz, 1H), 3.26 (td, *J* = 12.9, 2.4 Hz, 2H), 3.72 (d, *J* = 7.3 Hz, 2H), 4.29–4.38 (m, 2H), 5.90 (d, *J* = 8.1 Hz, 1H), 7.01–7.08 (m, 1H), 7.09–7.15 (m, 1H), 7.18–7.26 (m, 2H), 7.30 (d, *J* = 7.9 Hz, 1H). LC–MS *m/z* 352 [M + H]⁺.

1-(Cyclopropylmethyl)-4-[4-(3-fluorophenyl)-1-piperidyl]-2-oxo-pyridine-3-carbonitrile (23). Starting from **48b** (0.215 g, 0.61 mmol) and following the procedure described for **22**, compound **23** was obtained as a pale yellow solid (156 mg, 72%). ¹H NMR (400 MHz, CDCl₃) δ 0.33–0.46 (m, 2H), 0.56–0.70 (m, 2H), 1.16–1.28 (m, 1H), 1.85 (qd, *J* = 12.8, 3.8 Hz, 2H), 1.99–2.08 (m, 2H), 2.85 (tt, *J* = 12.1, 3.7 Hz, 1H), 3.19–3.30 (m, 2H), 3.74 (d, *J* = 7.0 Hz, 2H), 4.30–4.38 (m, 2H), 5.91 (d, *J* = 7.9 Hz, 1H), 6.91–6.98 (m, 2H), 7.02 (br d, *J* = 7.9 Hz, 1H), 7.27–7.35 (m, 1H), 7.32 (d, *J* = 7.9 Hz, 1H). LC–MS *m/z* 352 [M + H]⁺.

1-(Cyclopropylmethyl)-4-[4-(4-fluorophenyl)-1-piperidyl]-2-oxo-pyridine-3-carbonitrile (24). Triethylsilane (1.11 mL, 9.55 mmol) was added to a solution of **49** (0.351 g, 0.955 mmol) in CF₃CO₂H (0.5 mL, 6.49 mmol). The mixture was stirred at room temperature for 18 h and then diluted with CH₂Cl₂ (15 mL) and washed with 1 N NaOH (2 × 30 mL). The organic layer was separated, dried (Na₂SO₄), filtered, and concentrated in vacuo. The crude was purified by flash column chromatography (silica gel, MeOH–NH₃ in CH₂Cl₂, 0:100 to 2:98) to give **24** as a white solid (225 mg, 67%). mp 92.3 °C. ¹H NMR (400 MHz, CDCl₃) δ 0.26–0.39 (m, 2H), 0.48–0.61 (m, 2H), 1.11–1.21 (m, 1H), 1.75 (qd, *J* = 12.7, 3.7 Hz, 2H), 1.90–1.98 (m, 2H), 2.78 (tt, *J* = 12.1, 3.8 Hz, 1H), 3.13–3.23 (m, 2H), 3.67 (d, *J* = 7.0 Hz, 2H), 4.24–4.32 (m, 2H), 5.94 (d, *J* = 8.1 Hz, 1H), 6.92–6.99 (m, 2H), 7.10–7.18 (m, 2H), 7.36 (d, *J* = 7.9 Hz, 1H). LC–MS *m/z* 352 [M + H]⁺.

4-[4-(2-Chlorophenyl)-1-piperidyl]-1-(cyclopropylmethyl)-2-oxo-pyridine-3-carbonitrile (25). A solution of **48c** (0.68 g, 1.86 mmol) in MeOH (5 mL) and CH₃CO₂H (1 mL) was hydrogenated (atmospheric pressure) with PtO₂ (4 mg, 0.018 mmol) as a catalyst at

room temperature for 72 h. The mixture was filtered through a Celite pad, and the residue was washed with CH₂Cl₂. The filtrate was evaporated in vacuo, and the crude was purified by flash column chromatography (silica gel, silica gel, MeOH in CH₂Cl₂, 0:100 to 5:95) to give **25** as a white solid (289.6 mg, 42%). ¹H NMR (500 MHz, DMSO-*d*₆) δ 0.29–0.39 (m, 2H), 0.41–0.51 (m, 2H), 1.11–1.20 (m, 1H), 1.72 (qd, *J* = 12.6, 3.6 Hz, 2H), 1.89 (br d, *J* = 12.4 Hz, 2H), 3.24–3.32 (m, 3H), 3.63 (d, *J* = 6.9 Hz, 2H), 4.29 (br d, *J* = 13.6 Hz, 2H), 6.19 (d, *J* = 8.1 Hz, 1H), 7.25 (td, *J* = 7.8, 1.7 Hz, 1H), 7.33 (td, *J* = 7.5, 1.2 Hz, 1H), 7.40 (dd, *J* = 7.8, 1.7 Hz, 1H), 7.44 (dd, *J* = 7.9, 1.3 Hz, 1H), 7.71 (d, *J* = 8.1 Hz, 1H). LC–MS *m/z* 368 [M + H]⁺.

4-[4-(4-Chlorophenyl)-1-piperidyl]-1-(cyclopropylmethyl)-2-oxo-pyridine-3-carbonitrile (26). Starting from **41a** (0.35 g, 1.38 mmol) and following the procedure described for **10**, compound **26** was obtained as a solid (177.42 mg, 35%). ¹H NMR (400 MHz, CDCl₃) δ 0.15–0.27 (m, 2H), 0.38–0.51 (m, 2H), 0.98–1.10 (m, 1H), 1.65 (qd, *J* = 12.7, 3.9 Hz, 2H), 1.79–1.87 (m, 2H), 2.64 (tt, *J* = 12.1, 3.8 Hz, 1H), 3.01–3.11 (m, 2H), 3.56 (d, *J* = 7.3 Hz, 2H), 4.12–4.19 (m, 2H), 5.73 (d, *J* = 8.1 Hz, 1H), 6.97–7.03 (m, 2H), 7.11–7.18 (m, 3H). LC–MS *m/z* 368 [M + H]⁺.

1-(Cyclopropylmethyl)-2-oxo-4-[4-[3-(trifluoromethyl)-phenyl]-1-piperidyl]pyridine-3-carbonitrile (27). DIPEA (0.72 mL, 4.14 mmol) was added to a mixture of **41a** (0.35 g, 1.38 mmol) and 4-(3-trifluoromethyl-phenyl)-piperidine (0.41 g, 1.79 mmol) in CH₃CN (8 mL). The reaction mixture was heated at 170 °C for 35 min in a microwave oven. The mixture was washed with a saturated solution of NH₄Cl and extracted with CH₂Cl₂ (2 × 5 mL). The combined organic layers were dried over Na₂SO₄, filtered, and concentrated in vacuo. The crude was purified by flash column chromatography (silica gel, silica gel, MeOH–NH₃ in CH₂Cl₂, 0:100 to 1:99). Desired fractions were collected, and the solvent was evaporated to yield compound **27** (0.414 g, 75%) as a white solid. mp 111.9 °C. ¹H NMR (400 MHz, CDCl₃) δ 0.31–0.44 (m, 2H), 0.55–0.68 (m, 2H), 1.15–1.27 (m, 1H), 1.87 (qd, *J* = 12.8, 3.7 Hz, 2H), 2.00–2.09 (m, 2H), 2.90 (tt, *J* = 12.1, 3.7 Hz, 1H), 3.19–3.30 (m, 2H), 3.73 (d, *J* = 7.3 Hz, 2H), 4.29–4.39 (m, 2H), 5.91 (d, *J* = 7.9 Hz, 1H), 7.32 (d, *J* = 8.1 Hz, 1H), 7.39–7.56 (m, 4H). LC–MS *m/z* 402 [M + H]⁺.

1-(Cyclopropylmethyl)-4-[4-(2-methoxyphenyl)-1-piperidyl]-2-oxo-pyridine-3-carbonitrile (28). Starting from **41a** (0.35 g, 1.38 mmol) and 4-(2-methoxy-phenyl)-piperidine (0.342 g, 1.79 mmol) following the procedure described for **27**, compound **28** was obtained as a white solid (0.319 g, 64%). mp 148.1 °C. ¹H NMR (400 MHz, CDCl₃) δ 0.30–0.43 (m, 2H), 0.54–0.68 (m, 2H), 1.15–1.25 (m, 1H), 1.81 (qd, *J* = 12.6, 3.7 Hz, 2H), 1.95–2.03 (m, 2H), 3.21–3.32 (m, 3H), 3.72 (d, *J* = 7.3 Hz, 2H), 3.85 (s, 3H), 4.29–4.37 (m, 2H), 5.90 (d, *J* = 8.1 Hz, 1H), 6.88 (dd, *J* = 8.2, 1.1 Hz, 1H), 6.94 (td, *J* = 7.5, 1.0 Hz, 1H), 7.17 (dd, *J* = 7.6, 1.8 Hz, 1H), 7.19–7.25 (m, 1H), 7.29 (d, *J* = 7.9 Hz, 1H). LC–MS *m/z* 364 [M + H]⁺.

1-(Cyclopropylmethyl)-4-[4-(4-methoxyphenyl)-1-piperidyl]-2-oxo-pyridine-3-carbonitrile (29). Starting from **41a** (0.35 g, 1.38 mmol) and 4-(4-methoxy-phenyl)-piperidine (0.376 g, 1.66 mmol) following the procedure described for **27**, compound **29** was obtained as a white solid (0.284 g, 48%). mp 247.6 °C. ¹H NMR (500 MHz, CDCl₃) δ 0.32–0.43 (m, 2H), 0.56–0.66 (m, 2H), 1.16–1.25 (m, 1H), 1.81 (qd, *J* = 12.7, 3.6 Hz, 2H), 1.99 (br d, *J* = 12.1 Hz, 2H), 2.78 (tt, *J* = 12.1, 3.5 Hz, 1H), 3.22 (br t, *J* = 12.9 Hz, 2H), 3.72 (d, *J* = 7.2 Hz, 2H), 3.80 (s, 3H), 4.32 (br d, *J* = 13.3 Hz, 2H), 5.90 (d, *J* = 7.8 Hz, 1H), 6.87 (d, *J* = 8.7 Hz, 2H), 7.15 (d, *J* = 8.7 Hz, 2H), 7.30 (d, *J* = 7.8 Hz, 1H). LC–MS *m/z* 364 [M + H]⁺.

1-(Cyclopropylmethyl)-4-[4-(2,4-difluorophenyl)-1-piperidyl]-2-oxo-pyridine-3-carbonitrile (30). **48c** (0.9 g, 2.67 mmol) and 10% Pd/C (0.0028 g, 0.026 mmol) in MeOH (15 mL) were hydrogenated for 16 h. The crude was filtered over Celite and washed with MeOH, and the solution was dried over Na₂SO₄, filtered, and concentrated. The crude was purified by flash column chromatography (silica gel, silica gel, MeOH–NH₃ in CH₂Cl₂, 0:100 to 1:99). Desired fractions were collected, and the solvent was evaporated to yield compound **30** (0.614 g, 62%) as a white solid. mp 111.9 °C. ¹H NMR

(500 MHz, DMSO- d_6) δ 0.31–0.37 (m, 2H), 0.43–0.48 (m, 2H), 1.11–1.20 (m, 1H), 1.74 (qd, $J = 12.4$, 3.2 Hz, 2H), 1.81–1.88 (m, 2H), 3.14 (tt, $J = 12.1$, 3.8 Hz, 1H), 3.22–3.29 (m, 2H), 3.63 (d, $J = 7.2$ Hz, 2H), 4.26 (br d, $J = 13.6$ Hz, 2H), 6.18 (d, $J = 7.8$ Hz, 1H), 7.04 (td, $J = 8.5$, 2.3 Hz, 1H), 7.17–7.23 (m, 1H), 7.40 (td, $J = 8.5$, 6.9 Hz, 1H), 7.71 (d, $J = 8.1$ Hz, 1H). LC–MS m/z 370 [M + H]⁺.

1-(Cyclopropylmethyl)-4-[4-(2,6-difluorophenyl)-1-piperidyl]-2-oxo-pyridine-3-carbonitrile (31). Starting from 41a (0.35 g, 1.38 mmol) and 4-(2,6-difluoro-phenyl)-piperidine acetate (0.426 g, 1.65 mmol) following the procedure described for 27, compound 31 was obtained as a white solid (0.184 g, 31%). mp 144.2 °C. ¹H NMR (400 MHz, CDCl₃) δ 0.30–0.44 (m, 2H), 0.54–0.69 (m, 2H), 1.13–1.27 (m, 1H), 1.87 (br d, $J = 12.5$ Hz, 2H), 2.16–2.30 (m, 2H), 3.16–3.37 (m, 3H), 3.72 (d, $J = 7.2$ Hz, 2H), 4.34 (br d, $J = 13.6$ Hz, 2H), 5.90 (d, $J = 7.9$ Hz, 1H), 6.81–6.90 (m, 2H), 7.10–7.24 (m, 1H), 7.30 (d, $J = 7.9$ Hz, 1H). LC–MS m/z 370 [M + H]⁺.

1-(Cyclopropylmethyl)-4-[4-(3,5-difluorophenyl)-1-piperidyl]-2-oxo-pyridine-3-carbonitrile (32). Starting from 41a (0.35 g, 1.38 mmol) and 4-(3,5-difluoro-phenyl)-piperidine (0.3 g, 1.52 mmol) following the procedure described for 27, compound 32 was obtained as a white solid (0.28 g, 50%). ¹H NMR (500 MHz, DMSO- d_6) δ 0.29–0.39 (m, 2H), 0.41–0.51 (m, 2H), 1.10–1.19 (m, 1H), 1.70 (qd, $J = 12.6$, 3.6 Hz, 2H), 1.86–1.94 (m, 2H), 2.93 (tt, $J = 12.0$, 3.5 Hz, 1H), 3.17–3.25 (m, 2H), 3.63 (d, $J = 7.2$ Hz, 2H), 4.27 (br d, $J = 13.3$ Hz, 2H), 6.18 (d, $J = 8.1$ Hz, 1H), 7.04 (d, $J = 9.2$ Hz, 3H), 7.70 (d, $J = 7.8$ Hz, 1H). LC–MS m/z 370 [M + H]⁺.

3-Chloro-1-(cyclopropylmethyl)-4-(4-phenyl-1-piperidyl)pyridin-2-one (33). NCS (0.81 g, 6.09 mmol) was added to a mixture of 50a (1.89 g, 6.15 mmol) in CH₂Cl₂ (300 mL). The reaction mixture was stirred for 10 min at room temperature. The mixture was washed with a saturated solution of NaHCO₃ and extracted with CH₂Cl₂ (2 × 10 mL). The combined organic layers were dried over Na₂SO₄, filtered, and concentrated in vacuo. The crude was purified by flash column chromatography (silica gel, silica gel, MeOH–NH₃ in CH₂Cl₂, 0:100 to 3:97). Desired fractions were collected, and the solvent was evaporated to yield compound 33 (1.88 g, 85%) as a white solid. ¹H NMR (400 MHz, CDCl₃) δ 0.31–0.45 (m, 2H), 0.53–0.67 (m, 2H), 1.20–1.31 (m, 1H), 1.85–1.99 (m, 4H), 2.64–2.76 (m, 1H), 2.86–2.99 (m, 2H), 3.77–3.87 (m, 2H), 3.81 (d, $J = 7.2$ Hz, 2H), 6.05 (d, $J = 7.6$ Hz, 1H), 7.19–7.29 (m, 4H), 7.29–7.37 (m, 2H). LC–MS m/z 343 [M + H]⁺.

3-Trifluoromethyl-1-(cyclopropylmethyl)-4-(4-phenyl-1-piperidyl)pyridin-2-one (34). To a solution of 46 (0.3 g, 1.01 mmol) in toluene (7 mL) were added 4-phenylpiperidine (0.33 g, 2.02 mmol), Pd(OAc)₂ (0.012 g, 0.005 mmol), NaO^tBu (0.24 g, 2.52 mmol), and BINAP (0.05 g, 0.08 mmol). The mixture was heated at 100 °C for 16 h in a sealed tube. The cooled mixture was partitioned between water and EtOAc. The crude was extracted with EtOAc (3 × 5 mL), and the combined organic layers were dried (Na₂SO₄) and concentrated in vacuo. The crude was purified by flash column chromatography (silica gel, silica gel, MeOH in CH₂Cl₂, 0:100 to 4:96). Compound 34 was obtained as white solid (0.11 g, 31%). mp 177.2 °C. ¹H NMR (500 MHz, CDCl₃) δ 0.33–0.38 (m, 2H), 0.45–0.50 (m, 2H), 1.13–1.22 (m, 1H), 1.64–1.75 (m, 2H), 1.64–1.75 (m, 2H), 1.84 (br d, $J = 11.0$ Hz, 2H), 2.73–2.80 (m, 1H), 3.14 (br t, $J = 12.1$ Hz, 2H), 3.59 (br d, $J = 13.0$ Hz, 2H), 3.65 (d, $J = 7.2$ Hz, 2H), 6.21 (d, $J = 7.8$ Hz, 1H), 7.19–7.23 (m, 1H), 7.24–7.29 (m, 2H), 7.73 (d, $J = 7.8$ Hz, 1H). LC–MS m/z 377 [M + H]⁺.

3-Chloro-1-isobutyl-4-(4-phenyl-1-piperidyl)pyridin-2-one (35). Starting from 50b (0.35 g, 1.38 mmol) and *N*-chlorosuccinimide (0.62 g, 4.65 mmol) following the procedure described for 33, compound 35 was obtained as a white solid (1.42 g, 83%). ¹H NMR (400 MHz, CDCl₃) δ 0.94 (d, $J = 6.7$ Hz, 6H), 1.86–1.99 (m, 4H), 2.21 (dq, $J = 13.7$, 6.9 Hz, 1H), 2.65–2.76 (m, 1H), 2.88–2.97 (m, 2H), 3.74 (d, $J = 7.4$ Hz, 2H), 3.80–3.87 (m, 2H), 6.02 (d, $J = 7.6$ Hz, 1H), 7.07 (d, $J = 7.6$ Hz, 1H), 7.20–7.29 (m, 3H), 7.31–7.38 (m, 2H). LC–MS m/z 345 [M + H]⁺.

3-Chloro-1-butyl-4-(4-phenyl-1-piperidyl)pyridin-2-one (36). Starting from 50c (0.43 g, 1.40 mmol) and *N*-chlorosuccinimide (0.19 g, 1.4 mmol) following the procedure described for 33, compound 36

was obtained as a white solid (0.39 g, 82%). mp 149.4 °C. ¹H NMR (400 MHz, CDCl₃) δ 0.95 (t, $J = 7.3$ Hz, 3H), 1.31–1.42 (m, 2H), 1.68–1.78 (m, 2H), 1.85–1.98 (m, 4H), 2.64–2.73 (m, 1H), 2.87–2.98 (m, 2H), 3.82 (brd, $J = 12.1$ Hz, 2H), 3.93 (t, $J = 7.3$, 2H), 6.03 (d, $J = 7.6$ Hz, 1H), 7.10 (d, $J = 7.6$ Hz, 1H), 7.19–7.28 (m, 3H), 7.29–7.37 (m, 2H). LC–MS m/z 345 [M + H]⁺.

1-Isobutyl-4-methoxy-2-oxo-1,2-dihydropyridine-3-carbonitrile (39b). Starting from isobutyl bromide 38b (11.5 mL, 103 mmol) and 37 (8 g, 53.3 mmol) and following the procedure described for synthesis of 39a,c,d,e,²⁹ compound 39b was obtained as a white solid (11.0 g, quantitative). ¹H NMR (400 MHz, CDCl₃) δ 0.93 (d, $J = 6.7$ Hz, 6H), 2.10–2.22 (m, 1H), 3.74 (d, $J = 7.4$ Hz, 2H), 4.00 (s, 3H), 6.05 (d, $J = 7.9$ Hz, 1H), 7.44 (d, $J = 7.6$ Hz, 1H). LC–MS m/z 207 [M + H]⁺.

1-(2-Cyclopropylethyl)-4-methoxy-2-oxo-1,2-dihydropyridine-3-carbonitrile (39f). Starting from 2-cyclopropylethyl bromide 38g (2.59 g, 17.3 mmol) and 37 (7.1 g, 19.0 mmol) and following the procedure as described for synthesis of 39a,c,d,e,²⁹ compound 39f was obtained as a white solid (2.63 g, 70%). ¹H NMR (500 MHz, CDCl₃) δ 0.00–0.06 (m, 2H), 0.42–0.53 (m, 2H), 0.57–0.66 (m, 1H), 1.64 (quin, $J = 6.72$ Hz, 2H), 3.99 (s, 3H), 4.01 (t, $J = 6.90$ Hz, 2H), 6.07 (d, $J = 7.80$ Hz, 1H), 7.56 (d, $J = 7.80$ Hz, 1H). LC–MS m/z 219 [M + H]⁺.

1-(4,4,4-Trifluorobutyl)-4-methoxy-2-oxo-1,2-dihydropyridine-3-carbonitrile (39g). Starting from 38g (0.107 mL, 0.867 mmol) and following the procedure as described for synthesis of 39a,c,d,e,²⁹ compound 39g was obtained as a white solid (0.142 g, 82%). ¹H NMR (400 MHz, CDCl₃) δ 1.98–2.08 (m, 2H), 2.10–2.24 (m, 2H), 3.99–4.04 (m, 2H), 4.02 (s, 3H), 6.13 (d, $J = 7.9$ Hz, 1H), 7.52 (d, $J = 7.6$ Hz, 1H). LC–MS m/z 261 [M + H]⁺.

1-Isobutyl-4-hydroxy-2-oxo-1,2-dihydropyridine-3-carbonitrile (40b). Starting from 39b (10.93 g, 53 mmol) and following the procedure as described for synthesis of 40a,c,d,e,²⁹ compound 40b was obtained as a white solid (4.83 g, 47%). ¹H NMR (400 MHz, DMSO- d_6) δ 0.83 (d, $J = 6.9$ Hz, 6H), 1.99 (s, 1H), 3.65 (d, $J = 7.4$ Hz, 2H), 6.04 (d, $J = 7.6$ Hz, 1H), 7.79 (d, $J = 7.6$ Hz, 1H), 12.69 (br s, 1H). LC–MS m/z 193 [M + H]⁺.

1-(2-Cyclopropylethyl)-4-hydroxy-2-oxo-1,2-dihydropyridine-3-carbonitrile (40f). Starting from 39f (2.63 g, 12 mmol) and following the procedure as described for synthesis of 39a,c,d,e,²⁹ compound 40f was obtained as a white solid (1.15 g, 47%). ¹H NMR (500 MHz, DMSO- d_6) δ –0.09–0.02 (m, 2H) 0.31–0.42 (m, 2H) 0.56–0.65 (m, 1H) 1.48 (q, $J = 7.13$ Hz, 2H) 3.89 (t, $J = 6.94$ Hz, 2H) 6.03 (d, $J = 7.80$ Hz, 1H) 7.84 (d, $J = 7.51$ Hz, 1H) 12.61 (br s, 1H). LC–MS m/z 205 [M + H]⁺.

1-(4,4,4-Trifluorobutyl)-4-hydroxy-2-oxo-1,2-dihydropyridine-3-carbonitrile (40g). Starting from 39g (6.8 g, 26.1 mmol) and following the procedure as described for synthesis of 39a,c,d,e,²⁹ compound 40g was obtained as a white solid (5.9 g, 92%). ¹H NMR (400 MHz, DMSO- d_6) δ 1.77–1.87 (m, 2H), 2.19–2.36 (m, 2H), 3.89 (t, $J = 7.3$ Hz, 2H), 6.06 (d, $J = 7.6$ Hz, 1H), 7.84 (d, $J = 7.6$ Hz, 1H), 12.69 (br s, 1H). LC–MS m/z 247 [M + H]⁺.

4-Bromo-1-isobutyl-2-oxo-1,2-dihydropyridine-3-carbonitrile (41b). Starting from 40b (4.83 g, 25.1 mmol) and following the procedure as described for synthesis of 41a,c,d,e,²⁹ compound 41b was obtained as a white solid (4.21 g, 66%). ¹H NMR (400 MHz, CDCl₃) δ 0.95 (d, $J = 6.7$ Hz, 6H), 2.11–2.23 (m, 1H), 3.76 (d, $J = 7.4$ Hz, 2H), 6.49 (d, $J = 7.2$ Hz, 1H), 7.33 (d, $J = 7.2$ Hz, 1H). LC–MS m/z 256 [M + H]⁺.

4-Bromo-1-(2-cyclopropylethyl)-2-oxo-1,2-dihydropyridine-3-carbonitrile (41f). Starting from 40f (1.15 g, 5.63 mmol) and following the procedure as described for synthesis of 41a,c,d,e,²⁹ compound 41f was obtained as a white solid (1.04 g, 69%). ¹H NMR (400 MHz, CDCl₃) δ 0.00–0.12 (m, 2H), 0.42–0.55 (m, 2H), 0.57–0.69 (m, 1H), 1.67 (q, $J = 7.1$ Hz, 2H), 4.04 (t, $J = 6.9$ Hz, 2H), 6.50 (d, $J = 7.2$ Hz, 1H), 7.43 (d, $J = 7.2$ Hz, 1H). LC–MS m/z 268 [M + H]⁺.

4-Bromo-1-(4,4,4-trifluorobutyl)-2-oxo-1,2-dihydropyridine-3-carbonitrile (41g). Starting from 40g (5.1 g, 20.7 mmol) and following the procedure as described for synthesis of 41a,c,d,e,²⁹ compound 41g was obtained as a white solid (5.2 g, 82%). ¹H NMR

(400 MHz, CDCl₃) δ 2.00–2.11 (m, 2H), 2.12–2.27 (m, 2H), 4.05 (t, $J = 7.3$ Hz, 2H), 6.58 (d, $J = 7.4$ Hz, 1H), 7.47 (d, $J = 7.2$ Hz, 1H). LC–MS m/z 310 [M + H]⁺.

4-Benzyloxy-1-cyclopropylmethyl-1H-pyridin-2-one (43a). Cyclopropylmethyl bromide **38a** (2.64 mL, 27.33 mmol) and K₂CO₃ (10.3 g, 74.52 mmol) was added to a solution of **42** (5 g, 24.84 mmol) in CH₃CN (200 mL). The mixture was stirred at reflux for 16 h. The cooled mixture was filtered through a Celite pad and concentrated in vacuo. The residue thus obtained was precipitated by treatment with diethyl ether. The resulting solid was filtered off and dried in the vacuum oven (50 °C) to yield **43a** (6.32 g, 98%). ¹H NMR (500 MHz, CDCl₃) δ 0.31–0.41 (m, 2H), 0.53–0.64 (m, 2H), 1.21 (m, $J = 7.80$ Hz, 1H), 3.74 (d, $J = 6.94$ Hz, 2H), 4.98 (s, 2H), 5.97 (dd, $J = 7.51, 2.60$ Hz, 1H), 5.99 (d, $J = 2.89$ Hz, 1H), 7.25 (d, $J = 7.51$ Hz, 1H), 7.31–7.42 (m, 5H). LC–MS m/z 258 [M + H]⁺.

4-Benzyloxy-1-isobutyl-1H-pyridin-2-one (43b). Starting from ^tbutyl bromide **38b** (5.89 mL, 54.66 mmol) and **42** (10 g, 49.69 mmol) and following the procedure described for **43a**, compound **43b** was obtained as a white solid (11.25 g, 88%). ¹H NMR (400 MHz, CDCl₃) δ 0.93 (d, $J = 6.7$ Hz, 6H), 2.09–2.21 (m, 1H), 3.67 (d, $J = 7.4$ Hz, 2H), 4.98 (s, 2H), 5.94 (dd, $J = 7.4, 2.8$ Hz, 1H), 5.99 (d, $J = 2.8$ Hz, 1H), 7.08 (d, $J = 7.4$ Hz, 1H), 7.32–7.43 (m, 5H). LC–MS m/z 258 [M + H]⁺.

4-Benzyloxy-1-butyl-1H-pyridin-2-one (43c). Starting from ⁿbutyl bromide **38c** (8.80 mL, 81.99 mmol) and **42** (15 g, 74.54 mmol) and following the procedure described for **43a**, compound **43c** was obtained as a white solid (13.5 g, 70%). ¹H NMR (360 MHz, CDCl₃) δ 0.93 (t, $J = 7.32$ Hz, 3H), 1.28–1.40 (m, 2H), 1.62–1.73 (m, 2H), 3.84 (t, $J = 7.32$ Hz, 2H), 4.95 (s, 2H), 5.93 (dd, $J = 7.32, 2.90$ Hz, 1H), 5.97 (d, $J = 2.93$ Hz, 1H), 7.11 (d, $J = 7.32$ Hz, 1H), 7.27–7.42 (m, 5H). LC–MS m/z 258 [M + H]⁺.

4-Benzyloxy-1-cyclopropylmethyl-3-iodo-1H-pyridin-2-one (44). NIS (2.64 g, 11.74 mmol) was added to a solution of **43a** (3 g, 11.74 mmol) in acetic acid (40 mL). The mixture was stirred at room temperature for 1 h. The mixture was concentrated in vacuo. The crude was purified by flash column chromatography (silica gel, silica gel, MeOH in CH₂Cl₂, 0:100 to 3:97) to give the desired product **44** (4.12 g, 92%). ¹H NMR (500 MHz, CDCl₃) δ 0.32–0.42 (m, 2H), 0.54–0.65 (m, 2H), 1.19–1.29 (m, 1H), 3.82 (d, $J = 7.2$ Hz, 2H), 5.24 (s, 2H), 6.00 (d, $J = 7.5$ Hz, 1H), 7.31–7.37 (m, 2H), 7.38–7.47 (m, 4H). LC–MS m/z 382 [M + H]⁺.

4-Benzylox-1-cyclopropylmethyl-3-trifluoromethyl-1H-pyridin-2-one (45). Methyl 2,2-difluoro-2-(fluorosulfonyl)acetate (0.67 mL, 5.24 mmol) and intermediate **44** were added to a solution of CuI (0.99 g, 5.24 mmol) in DMF (30 mL). The mixture was heated at 100 °C for 5 h. The cooled mixture was filtered through a Celite pad and concentrated in vacuo. The crude was purified by flash column chromatography (silica gel, DCM) to give the desired product **45** (0.76 g, 89%). ¹H NMR (500 MHz, CDCl₃) δ 0.30–0.41 (m, 2H), 0.56–0.67 (m, 2H), 1.16–1.27 (m, 1H), 3.75 (d, $J = 7.2$ Hz, 2H), 5.22 (s, 2H), 6.08 (d, $J = 7.8$ Hz, 1H), 7.31–7.43 (m, 5H), 7.52 (d, $J = 7.8$ Hz, 1H). LC–MS m/z 324 [M + H]⁺.

4-Bromo-1-(cyclopropylmethyl)-3-(trifluoromethyl)pyridin-2-one (46). A solution of **45** (2 g, 6.18 mmol) in ethanol (60 mL) was hydrogenated (atmospheric pressure) with Pd/C (400 mg) as a catalyst at room temperature for 2 h. The mixture was filtered through Celite pad, and the filtrate was evaporated in vacuo. The residue was dissolved in DMF (28 mL), and phosphorus oxybromide (3.54 g, 12.36 mmol) was added. The mixture was heated at 100 °C for 1 h. The cooled mixture was partitioned between water and EtOAc. After three extractions with EtOAc, the combined organic layers were dried (Na₂SO₄) and concentrated in vacuo. The crude was purified by flash column chromatography (silica gel, DCM) to yield **46** (0.769 g, 42%). ¹H NMR (400 MHz, CDCl₃) δ 0.33–0.49 (m, 2H), 0.57–0.73 (m, 2H), 1.18–1.31 (m, 1H), 3.79 (d, $J = 7.40$ Hz, 2H), 6.51 (d, $J = 7.17$ Hz, 1H), 7.47 (d, $J = 7.17$ Hz, 1H). LC–MS m/z 296 [M + H]⁺.

4-Bromo-1-(cyclopropylmethyl)pyridin-2-one (47a). Starting from **43a** (2.196 g, 8.6 mmol) and following the procedure described for **46**, compound **47a** was obtained (1.82 g, 93%). ¹H NMR (400 MHz, CDCl₃) δ 0.31–0.44 (m, 2H), 0.55–0.69 (m, 2H), 1.16–1.28

(m, 1H), 3.76 (d, $J = 7.2$ Hz, 2H), 6.34 (dd, $J = 7.2, 2.3$ Hz, 1H), 6.82 (d, $J = 2.1$ Hz, 1H), 7.26 (d, $J = 7.2$ Hz, 1H). LC–MS m/z 228 [M + H]⁺.

4-Bromo-1-isobutyl-pyridin-2-one (47b). Starting from **43b** (6.78 g, 26.35 mmol) and following the procedure described for **46**, compound **47b** was obtained (3.5 g, 58%). ¹H NMR (500 MHz, CDCl₃) δ 0.93 (d, $J = 6.6$ Hz, 6H), 2.10–2.20 (m, 1H), 3.70 (d, $J = 7.5$ Hz, 2H), 6.33 (dd, $J = 7.2, 2.3$ Hz, 1H), 6.85 (d, $J = 2.0$ Hz, 1H), 7.08 (d, $J = 7.2$ Hz, 1H). LC–MS m/z 230 [M + H]⁺.

4-Bromo-1-butyl-pyridin-2-one (47c). Starting from **43c** (2.19 g, 8.5 mmol) and following the procedure described for **46**, compound **47c** was obtained (1.82 g, 93%). ¹H NMR (400 MHz, CDCl₃) δ 0.95 (t, $J = 7.3$ Hz, 3H), 1.36 (dq, $J = 15.1, 7.4$ Hz, 2H), 1.66–1.75 (m, 2H), 3.89 (t, $J = 7.4$ Hz, 2H), 6.34 (dd, $J = 7.2, 2.1$ Hz, 1H), 6.84 (d, $J = 2.3$ Hz, 1H), 7.14 (d, $J = 7.2$ Hz, 1H). LC–MS m/z 230 [M + H]⁺.

1-(Cyclopropylmethyl)-4-[4-(2-fluorophenyl)-3,6-dihydro-2H-pyridin-1-yl]-2-oxo-pyridine-3-carbonitrile (48a). Starting from **41a** (0.23 g, 0.91 mmol) and 4-(2-fluorophenyl)-1,2,3,6-tetrahydropyridine (0.2 g, 1.13 mmol) and following the procedure described for **10**, compound **48a** was obtained as a white solid (263 mg, 83%). ¹H NMR (400 MHz, CDCl₃) δ 0.30–0.43 (m, 2H), 0.53–0.66 (m, 2H), 1.14–1.26 (m, 1H), 2.71–2.78 (m, 2H), 3.72 (d, $J = 7.2$ Hz, 2H), 3.91 (t, $J = 5.5$ Hz, 2H), 4.32 (br q, $J = 2.6$ Hz, 2H), 5.95 (d, $J = 8.1$ Hz, 1H), 5.98–6.02 (m, 1H), 7.02–7.08 (m, 1H), 7.10–7.15 (m, 1H), 7.22–7.28 (m, 2H), 7.35 (d, $J = 7.9$ Hz, 1H). LC–MS m/z 350 [M + H]⁺.

1-(Cyclopropylmethyl)-4-[4-(3-fluorophenyl)-3,6-dihydro-2H-pyridin-1-yl]-2-oxo-pyridine-3-carbonitrile (48b). Starting from **41a** (0.23 g, 0.91 mmol) and 4-(3-fluorophenyl)-1,2,3,6-tetrahydropyridine (0.2 g, 1.13 mmol) and following the procedure described for **6**, compound **48b** was obtained as a white solid (246 mg, 77%). ¹H NMR (400 MHz, CDCl₃) δ 0.30–0.43 (m, 2H), 0.53–0.67 (m, 2H), 1.14–1.25 (m, 1H), 2.71–2.78 (m, 2H), 3.72 (d, $J = 7.2$ Hz, 2H), 3.93 (t, $J = 5.5$ Hz, 2H), 4.30 (q, $J = 2.7$ Hz, 2H), 5.93 (d, $J = 8.1$ Hz, 1H), 6.09–6.13 (m, 1H), 6.98 (tdd, $J = 8.3, 2.5, 0.9$ Hz, 1H), 7.08 (dt, $J = 10.5, 2.2$ Hz, 1H), 7.15–7.19 (m, 1H), 7.31 (td, $J = 8.0, 6.0$ Hz, 1H), 7.34 (d, $J = 8.1$ Hz, 1H). LC–MS m/z 350 [M + H]⁺.

4-[4-(2-Chlorophenyl)-3,6-dihydro-2H-pyridin-1-yl]-1-(cyclopropylmethyl)-2-oxo-pyridine-3-carbonitrile (48c). Starting from **41a** (0.47 g, 1.88 mmol) and 4-(2-chlorophenyl)-1,2,3,6-tetrahydropyridine (0.4 g, 2.07 mmol) and following the procedure described for **10**, compound **48c** was obtained as a white solid (680 mg, 100%). ¹H NMR (500 MHz, CDCl₃) δ 0.32–0.42 (m, 2H), 0.54–0.65 (m, 2H), 1.16–1.24 (m, 1H), 2.65–2.71 (m, 2H), 3.72 (d, $J = 7.2$ Hz, 2H), 3.91 (t, $J = 5.5$ Hz, 2H), 4.31 (br q, $J = 2.9$ Hz, 2H), 5.72–5.75 (m, 1H), 5.94 (d, $J = 7.8$ Hz, 1H), 7.16–7.20 (m, 1H), 7.21–7.26 (m, 2H), 7.34 (d, $J = 8.1$ Hz, 1H), 7.36–7.39 (m, 1H). LC–MS m/z 366 [M + H]⁺.

1-(Cyclopropylmethyl)-4-[4-(2,4-difluorophenyl)-3,6-dihydro-2H-pyridin-1-yl]-2-oxo-pyridine-3-carbonitrile (48d). Starting from **41a** (0.67 g, 2.67 mmol) and 4-(2,4-difluorophenyl)-1,2,3,6-tetrahydropyridine (0.57 g, 2.94 mmol) and following the procedure described for **10**, compound **48d** was obtained as a white solid (900 mg, 92%). ¹H NMR (500 MHz, CDCl₃) δ 0.32–0.42 (m, 2H), 0.54–0.65 (m, 2H), 1.15–1.24 (m, 1H), 2.71 (br s, 2H), 3.72 (d, $J = 7.2$ Hz, 2H), 3.90 (t, $J = 5.5$ Hz, 2H), 4.30 (br q, $J = 2.6$ Hz, 2H), 5.93 (d, $J = 8.1$ Hz, 1H), 5.95–5.98 (m, 1H), 6.81 (ddd, $J = 11.2, 8.7, 2.6$ Hz, 1H), 6.84–6.89 (m, 1H), 7.23 (td, $J = 8.7, 6.4$ Hz, 1H), 7.34 (d, $J = 7.8$ Hz, 1H). LC–MS m/z 368 [M + H]⁺.

1-(Cyclopropylmethyl)-4-[4-(4-fluorophenyl)-4-hydroxy-1-piperidyl]-2-oxo-pyridine-3-carbonitrile (49). To a solution of **46** (0.77 g, 1.88 mmol) in CH₃CN (10 mL) were added 4-(4-fluorophenyl)-piperidin-4-ol (0.369 g, 1.89 mmol) and DIPEA (0.697 mL, 4 mmol). The mixture was heated under microwave irradiation at 140 °C for 30 min. The cooled mixture was evaporated in vacuo. The residue was taken up in CH₂Cl₂ and washed with saturated solution of NaHCO₃. The combined organic layers were dried over Na₂SO₄ and concentrated in vacuo. The crude was purified by flash column chromatography (silica gel, silica gel, MeOH–NH₃ in CH₂Cl₂, 0:100 to 2:98); compound **49** was obtained as a white solid (0.53 g, 73%).

¹H NMR (500 MHz, CDCl₃) δ 0.32–0.42 (m, 2H), 0.56–0.67 (m, 2H), 1.15–1.24 (m, 1H), 1.60 (br s, 1H), 1.90–1.97 (m, 2H), 2.20 (td, *J* = 13.2, 4.2 Hz, 2H), 3.66 (td, *J* = 12.9, 2.2 Hz, 2H), 3.72 (d, *J* = 6.9 Hz, 2H), 4.09–4.16 (m, 2H), 5.91 (d, *J* = 8.1 Hz, 1H), 7.07 (br t, *J* = 8.7 Hz, 2H), 7.30 (d, *J* = 7.8 Hz, 1H), 7.44–7.51 (m, 2H). LC–MS *m/z* 368 [M + H]⁺.

1-(Cyclopropylmethyl)-4-(4-phenyl-1-piperidyl)pyridin-2-one (50a). To a solution of 47a (0.4 g, 1.58 mmol) in toluene (5 mL) were added 4-phenylpiperidine (0.509 g, 3.16 mmol), Pd(OAc)₂ (0.017 g, 0.079 mmol), NaO^tBu (0.38 g, 3.95 mmol), and BINAP (0.073 g, 0.11 mmol). The mixture was heated at 100 °C for 16 h in a sealed tube. The cooled mixture was partitioned between water and EtOAc. The crude was extracted with EtOAc (3 × 5 mL), and the combined organic layers were dried (Na₂SO₄) and concentrated in vacuo. The crude was purified by flash column chromatography (silica gel, silica gel, MeOH–NH₃ in CH₂Cl₂, 0:100 to 1:99); compound 50a was obtained as brown oil (0.48 g, 98%). ¹H NMR (500 MHz, CDCl₃) δ 0.31–0.42 (m, 2H), 0.53–0.64 (m, 2H), 1.19–1.28 (m, 1H), 1.77 (qd, *J* = 12.7, 3.9 Hz, 2H), 1.89–1.96 (m, 2H), 2.76 (tt, *J* = 12.1, 3.6 Hz, 1H), 2.96 (td, *J* = 12.8, 2.2 Hz, 2H), 3.73 (d, *J* = 7.2 Hz, 2H), 3.90–3.97 (m, 2H), 5.82 (d, *J* = 2.9 Hz, 1H), 5.98 (dd, *J* = 7.8, 2.9 Hz, 1H), 7.17–7.26 (m, 4H), 7.30–7.35 (m, 2H). LC–MS *m/z* 309 [M + H]⁺.

1-Isobutyl-4-(4-phenyl-1-piperidyl)pyridin-2-one (50b). To a solution of 47b (2 g, 8.69 mmol) in toluene (35 mL) were added 4-phenylpiperidine (1.962 g, 12.16 mmol), Pd(OAc)₂ (0.098 g, 0.43 mmol), NaO^tBu (2.088 g, 21.72 mmol), and 2,2'-bis (diphenylphosphino)-1,1'-binaphthyl (0.406 g, 0.652 mmol). The mixture was heated at 100 °C for 16 h in a sealed tube. The cooled mixture was partitioned between water and EtOAc. The crude was extracted with EtOAc (3 × 5 mL), and the combined organic layers were dried (Na₂SO₄) and concentrated in vacuo. The crude was purified by flash column chromatography (silica gel, silica gel, MeOH in CH₂Cl₂, 0:100 to 4:96); compound 50b was obtained as a white solid (1.9 g, 65%). ¹H NMR (500 MHz, CDCl₃) δ 0.93 (d, *J* = 6.6 Hz, 6H), 1.76 (qd, *J* = 12.8, 3.5 Hz, 2H), 1.87–1.94 (m, 2H), 2.11–2.21 (m, 1H), 2.74 (tt, *J* = 12.1, 3.5 Hz, 1H), 2.94 (td, *J* = 12.8, 2.5 Hz, 2H), 3.64 (d, *J* = 7.5 Hz, 2H), 3.88–3.95 (m, 2H), 5.78 (d, *J* = 2.9 Hz, 1H), 5.93 (dd, *J* = 7.8, 2.6 Hz, 1H), 7.02 (d, *J* = 7.5 Hz, 1H), 7.17–7.25 (m, 3H), 7.28–7.34 (m, 2H). LC–MS *m/z* 311 [M + H]⁺.

1-Butyl-4-(4-phenyl-1-piperidyl)pyridin-2-one (50c). To a solution of 47c (2 g, 8.69 mmol) in toluene (75 mL) were added 4-phenylpiperidine (2.1 g, 13.038 mmol), Pd(OAc)₂ (0.98 g, 0.435 mmol), NaO^tBu (2.09 g, 21.73 mmol), and BINAP (0.406 g, 0.652 mmol). The mixture was heated at 100 °C for 16 h in a sealed tube. The cooled mixture was partitioned between water and EtOAc. The crude was extracted with EtOAc (3 × 5 mL), and the combined organic layers were dried over Na₂SO₄ and concentrated in vacuo. The crude was purified by flash column chromatography (silica gel, silica gel, MeOH–NH₃ in CH₂Cl₂, 0:100 to 4:96); compound 50c was obtained (1.8 g, 66%). ¹H NMR (400 MHz, CDCl₃) δ 0.95 (t, *J* = 7.4 Hz, 3H), 1.31–1.43 (m, 2H), 1.65–1.82 (m, 4H), 1.86–1.95 (m, 2H), 2.74 (tt, *J* = 12.1, 3.7 Hz, 1H), 2.94 (td, *J* = 12.8, 2.5 Hz, 2H), 3.84 (t, *J* = 7.4 Hz, 2H), 3.88–3.95 (m, 2H), 5.79 (d, *J* = 2.8 Hz, 1H), 5.95 (dd, *J* = 7.7, 2.9 Hz, 1H), 7.06 (d, *J* = 7.6 Hz, 1H), 7.17–7.25 (m, 3H), 7.28–7.35 (m, 2H). LC–MS *m/z* 311 [M + H]⁺.

1-Isopentyl-2-oxo-4-(2-phenylethynyl)pyridine-3-carbonitrile (51). To a solution of 41d (0.15 g, 0.6 mmol) in THF (6 mL) were added phenylacetylene (0.064 mL, 0.6 mmol), PdCl₂(PPh₃)₂ (0.02 g, 0.028 mmol), Et₃N (0.0787 mL, 2.2 mmol), and PPh₃ (0.0037 g, 0.014 mmol). The mixture was degassed for 5 min, and then CuI (0.0013 g, 0.007 mmol) was added. The mixture was heated at 90 °C for 10 h in a sealed tube. The mixture was cooled to room temperature and treated with aqueous Na₂S₂O₄ and CH₂Cl₂. The layers were separated, the organic layer was washed with a saturated aqueous solution of NaHCO₃, and the combined organic layers were dried (Na₂SO₄) and concentrated in vacuo. The crude was purified by automated flash column chromatography over silica gel (silica gel, silica gel, MeOH–NH₃ in CH₂Cl₂, 0:100 to 2:98); compound 51 was obtained (0.097 g, 60%). ¹H NMR (400 MHz, CDCl₃) δ 0.97 (d, *J* =

6.2 Hz, 6H), 1.56–1.71 (m, 3H), 3.94–4.01 (m, 2H), 6.36 (d, *J* = 6.8 Hz, 1H), 7.36–7.47 (m, 3H), 7.53 (d, *J* = 7.0 Hz, 1H), 7.59–7.65 (m, 2H). LC–MS *m/z* 291 [M + H]⁺.

Biology. Membrane Preparation. CHO cells expressing the human mGlu2 receptor were grown until they were 80% confluent, washed in ice-cold phosphate buffered saline, and stored at –20 °C until membrane preparation. After thawing, cells were suspended in 50 mM Tris–HCl, pH 7.4, and collected through centrifugation for 10 min at 23 500g at 4 °C. Cells were lysed in 5 mM hypotonic Tris–HCl, pH 7.4, and after recentrifugation for 20 min at 30 000g at 4 °C, the pellet was homogenized with an Ultra Turrax homogenizer in 50 mM Tris–HCl, pH 7.4. Protein concentrations were measured by the Bio-Rad protein assay using bovine serum albumin as standard.

[³⁵S]GTPγS Binding Assay. For [³⁵S]GTPγS measurements, compound and glutamate were diluted in buffer containing 10 mM HEPES acid, 10 mM HEPES salt, pH 7.4, containing 100 mM NaCl, 3 mM MgCl₂, and 10 μM GDP. Membranes were thawed on ice and diluted in the same buffer, supplemented with 14 μg/mL saponin (final assay concentration of 2 μg/mL saponin). Final assay mixtures contained 7 μg of membrane protein and were preincubated with compound alone (determination of agonist effects) or together with an EC₂₀ concentration (4 μM) of glutamate (determination of PAM effects) for 30 min at 30 °C. [³⁵S]GTPγS was added at a final concentration of 0.1 nM and incubated for another 30 min at 30 °C. Reactions were terminated by rapid filtration through Unifilter-96 GF/B filter plates (Packard) using a 96-well Packard filtermate harvester. Filters were washed six times with ice-cold 10 mM NaH₂PO₄/10 mM Na₂HPO₄, pH 7.4, and filter-bound radioactivity was counted in a microplate scintillation and luminescence counter from Packard.

Data Analysis. Data were processed using an internal software interface and were calculated as the percent of the control agonist challenge. Sigmoid concentration–response curves plotting these percentages versus the log concentration of the test compound were analyzed using nonlinear regression analysis. The EC₅₀ is the concentration of a compound that causes a half-maximal potentiation of the glutamate response. The pEC₅₀ values are calculated as the –log EC₅₀ (wherein EC₅₀ is expressed in mol L^{–1}).

Patch-Clamp Assay. Experiments were performed using HEK293 cells stably expressing the hERG potassium channel. Cells were grown at 37 °C and 5% CO₂ in culture flasks in MEM medium supplemented with 10% heat-inactivated fetal bovine serum, 1% L-glutamine–penicillin–streptomycin solution, 1% nonessential amino acids (100×), 1% sodium pyruvate (100 mM), and 0.8% Geneticin (50 mg/mL). Before use, the cells were subcultured in MEM medium in the absence of 5 mL of L-glutamine–penicillin–streptomycin. For use in the automated patch-clamp system PatchXpress 7000A (Axon Instruments), cells were harvested to obtain cell suspension of single cells. The extracellular solution contained the following (mM): 150 NaCl, 4 KCl, 1 MgCl₂, 1.8 CaCl₂, 10 HEPES, 5 glucose (pH 7.4 with NaOH). The pipette solution contained the following (mM): 120 KCl, 10 HEPES, 5 EGTA, 4 ATP–Mg₂, 2 MgCl₂, 0.5 CaCl₂ (pH 7.2 with KOH). Patch-clamp experiments were performed in the voltage-clamp mode, and whole-cell currents were recorded with an automated patch-clamp assay utilizing the PatchXpress 7000A system (Axon Instruments). Current signals were amplified and digitized by a multiclamp amplifier, stored, and analyzed by using the PatchXpress and DataXpress software and Igor 5.0 (Wavemetrics). The holding potential was –80 mV. The hERG current (K⁺-selective outward current) was determined as the maximal tail current at –40 mV after a 2 s depolarization to +60 mV. The pulse cycling rate was 15 s. Before each test pulse, a short pulse (0.5 s) from the holding potential to –60 mV was given to determine (linear) leak current. After establishment of whole-cell configuration and a stability period, the vehicle was applied for 5 min followed by the test substance at increasing concentrations of 10^{–7}, 3 × 10^{–7}, and 3 × 10^{–6} M. Each concentration of the test substance was applied twice. The effect of each concentration was determined after 5 min as an average current of three sequential voltage pulses. To determine the extent of block, the residual current was compared with vehicle pretreatment.

Sleep–Wake EEG: Animals, Drug Treatment, and Experimental Procedure. All in vivo experimental procedures were performed according to the applicable European Communities Council Directive of November 24, 1986 (86/609/EEC) and approved by the Animal Care and Use Committee of Janssen Pharmaceutical Companies of Johnson & Johnson and by the local ethical committee. Male Sprague–Dawley rats (Charles River, France) weighing 250–300 g were used. Animals were chronically implanted with electrodes for recording the cortical electroencephalogram (EEG), electrical neck muscle activity (EMG), and ocular movements (EOG). All animals were housed in individually ventilated cages under environmentally controlled conditions (ambient temperature, 22 °C; humidity, 60%) on a 12 h light/dark cycle (lights on from 12:00 a.m. to 12:00 p.m., illumination intensity of ~100 lx). The animals had free access to food and tap water. The effects of the tested molecule and vehicle on sleep–wake distribution during the lights-on period were investigated in 16 rats ($n = 8$ each group). Two EEG recording sessions were performed: the first recording session started at 13:30 h and lasted 20 h following oral administration of saline. The second recording session was performed during the same consecutive circadian time and for the same duration following administration of either vehicle (20% CD + 2H2T) or tested compound. Sleep polysomnographic variables were determined offline as described elsewhere using a sleep stages analyzer, scoring each 2 s epoch before averaging stages over 30 min periods. Sleep–wake state classifications were assigned on the basis of the combination of dynamics of five EEG frequency domains, integrated EMG, EOG, and body activity level: active wake (AW); passive wake (PW); intermediate stage (pre-REM transients); rapid eye movement sleep (REM); light non-REM sleep (ISWS); deep non-REM sleep (dSWS). Different sleep–wake parameters were investigated over 20 h postadministration, and time spent in each vigilance state, sleep parameters, latencies for first REM sleep period and the number of transitions between states were determined.

Statistical Analysis. Time spent in each vigilance state (AW, PW, ISWS, dSWS, IS, and REMS) was expressed as a percentage of the recording period. A statistical analysis of the obtained data was carried out by a nonparametric analysis of variance of each 30 min period, followed by a Wilcoxon–Mann–Whitney rank sum test of comparisons with the control group.

AUTHOR INFORMATION

Corresponding Author

*Tel: +34 925 245767. Fax: +34 925 245771. E-mail: jcid@its.jnj.com.

Notes

The authors declare no competing financial interest.

ACKNOWLEDGMENTS

The authors thank Addex Therapeutics for its collaboration on the mGlu2PAM discovery program, members of the purification and analysis team from Toledo, the biology and ADMET team from Janssen R & D, and Lieve Heylen, Heidi Szel, and Ria Wouters for technical assistance.

ABBREVIATIONS USED

AcOH, acetic acid; ADME, absorption, distribution, metabolism, excretion; AUC, area under the curve; AW, active wake; BBB, blood–brain barrier; BINAP, 2,2'-bis-(diphenylphosphino)-1,1'-binaphthyl; B/P, brain plasma ratio; Cl, clearance; C_{max} , maximum plasma concentrations; CNS, central nervous system; CV, cardiovascular; dSWS, deep non-REM sleep; DCM, dichloromethane; DIPEA, diisopropylethylamine; DMF, dimethylformamide; DMSO, dimethyl sulfoxide; EEG, electroencephalogram; EMG, electrical neck muscle activity; EOG, ocular movement; EtOAc, ethyl acetate;

GCMS, gas chromatography mass spectrometry; GPCR, G-protein-coupled receptor; h, hours; HLM, human liver microsome; HP- β -CD, 2-hydroxypropyl- β -cyclodextrin; HTS, high-throughput screening; iGlu, ionotropic glutamate; iv, intravenous; LAD, lowest active dose; LC–MS, liquid chromatography combined with mass spectrometry; mGlu2, metabotropic glutamate 2; min, minutes; ISWS, light non-REM sleep; MDD, major depressive disorder; MeOH, methanol; mp, melting point; MW, molecular weight; NCS, N-chlorosuccinimide; ND, not determined; NM, not measurable; NIS, N-iodosuccinimide; NMDA, N-methyl-D-aspartate; NMR, nuclear magnetic resonance; NOEL, no effect level; NT, not tested; PAM, positive allosteric modulator; PCP, phencyclidine; PK, pharmacokinetics; po, per oral; PW, passive wake; SAR, structure–activity relationship; SEM, standard error of mean; po, oral; REM, rapid eye movement; RLM, rat liver microsome; ROL, REM sleep onset latency; rt, room temperature; RP-HPLC, reverse-phase high-performance liquid chromatography; sc, subcutaneous; SD, standard deviation; sw-EEG, sleep–wake electroencephalogram; TFA, trifluoroacetic acid; THF, tetrahydrofuran; TLC, thin-layer chromatography; TPSA, total polar surface area; V_d , volume of distribution

REFERENCES

- (1) Kew, J. N.; Kemp, J. A. Ionotropic and metabotropic glutamate receptor, structure and pharmacology. *Psychopharmacology* **2005**, *182*, 320.
- (2) Pin, J. P.; Galvez, T.; Prezeau, L. Evolution, structure, and activation mechanism of family 3/C G-protein-coupled receptors. *Pharmacol. Ther.* **2003**, *98*, 325–354.
- (3) Brauner-Osborne, H.; Wellendorph, P.; Jensen, A. A. Structure, pharmacology and therapeutic prospects of family C G-protein coupled receptors. *Curr. Drug Targets* **2007**, *8*, 169–184.
- (4) Lavreysen, H.; Dautzenberg, F. Therapeutic potential of group III metabotropic glutamate receptors. *Curr. Med. Chem.* **2008**, *15*, 671–684.
- (5) Niswender, C. M.; Conn, P. J. Metabotropic glutamate receptors: physiology, pharmacology, and disease. *Annu. Rev. Pharmacol. Toxicol.* **2010**, *50*, 295–322.
- (6) Wright, R. A.; Johnson, B. G.; Zhang, C.; Salhoff, C.; Kingston, A. E.; Calligaro, D. O.; Monn, J. A.; Schoepp, D. D.; Marek, G. J. CNS distribution of metabotropic glutamate 2 and 3 receptors: transgenic mice and [³H]LY459477 autoradiography. *Neuropharmacology* **2013**, *66*, 89–98.
- (7) Schoepp, D. D.; Marek, G. J. Preclinical pharmacology of mGluR2/3 receptor agonists: novel agents for schizophrenia? *Curr. Drug Targets: CNS Neurol. Disord.* **2002**, *1*, 215–225.
- (8) Moghaddam, B.; Adams, B. W. Reversal of phencyclidine effects by a group II metabotropic glutamate receptor agonist in rats. *Science* **1998**, *281*, 477–484.
- (9) Cartmell, J.; Monn, J. A.; Schoepp, D. D. The metabotropic glutamate 2/3 receptor agonists LY354740 and LY379268 selectively attenuate phencyclidine versus d-amphetamine motor behaviors in rats. *J. Pharmacol. Exp. Ther.* **1999**, *291*, 161–170.
- (10) Patil, S. T.; Zhang, L.; Martenyi, F.; Lowe, S. L.; Jackson, K. A.; Andreev, B. V.; Avedisova, A. S.; Bardenstein, L. M.; Gurovich, I. Y.; Morozova, M. A.; Mosolov, S. N.; Neznanov, N. G.; Reznik, A. M.; Smulevich, A. B.; Tochilov, V. A.; Johnson, B. G.; Monn, J. A.; Schoepp, D. D. Activation of mGlu2/3 receptors as a new approach to treat schizophrenia: a randomized Phase 2 clinical trial. *Nat. Med.* **2007**, *13*, 1102–1107.
- (11) Kinon, B. J.; Zhang, L.; Millen, B. A.; Osuntokun, O. O.; Williams, J. E.; Kollack-Walker, S.; Kimberley, J.; Ludmila, K.; Natalia, J. A multicenter, inpatient, phase 2, double-blind, placebo-controlled dose-ranging study of LY2140023 monohydrate in patients with DSM-IV schizophrenia. *J. Clin. Psychopharmacol.* **2011**, *31*, 349–355.

- (12) Kinon, B. J.; Gómez, J. C. Clinical development of pomaglutetad methionil: a non-dopaminergic treatment for schizophrenia. *Neuropharmacology* **2013**, *66*, 82–86.
- (13) *Lilly Stops Phase III development of pomaglutetad methionil for the treatment of schizophrenia based on efficacy results*; Eli Lilly and Co.: Indianapolis, IN, 2012; <https://investor.lilly.com/releasedetail.cfm?ReleaseID=703018>.
- (14) Schoepp, D. D.; Wright, R. A.; Levine, L. R.; Gaydos, B.; Potter, W. Z. LY354740, an mGlu2/3 receptor agonist as a novel approach to treat anxiety/stress. *Stress* **2003**, *6*, 189–197.
- (15) Woolley, M. L.; Pemberton, D. J.; Bate, S.; Corti, C.; Jones, D. N. C. The mGlu2 but not the mGlu3 receptor mediates the actions of the mGluR2/3 agonist, LY379268, in mouse models predictive of antipsychotic activity. *Psychopharmacology* **2008**, *196*, 431–440.
- (16) Fell, M. J.; Svensson, K. A.; Johnson, B. G.; Schoepp, D. D. Evidence for the role of mGlu2 not mGlu3 receptors in the preclinical antipsychotic pharmacology of the mGlu2/3 receptor agonist LY404039. *J. Pharmacol. Exp. Ther.* **2008**, *326*, 209–217.
- (17) Galici, R.; Echemendia, N. G.; Rodriguez, A. L.; Conn, P. J. A selective allosteric potentiator of metabotropic glutamate (mGlu) 2 receptors has effects similar to an orthosteric mGlu2/3 receptor agonist in mouse models predictive of antipsychotic activity. *J. Pharmacol. Exp. Ther.* **2005**, *315*, 1181–1187.
- (18) Conn, P. J.; Christopoulos, A.; Lindsley, C. W. Allosteric modulators of GPCRs: a novel approach for the treatment of CNS disorders. *Nat. Rev. Drug. Discovery* **2009**, *8*, 41–54.
- (19) Pin, J. P.; Parmentier, M.-L.; Prezeau, L. Positive allosteric modulators for g-aminobutyric acidB receptors open new routes for the development of drugs targeting family 3 G-protein-coupled receptors. *Mol. Pharmacol.* **2001**, *60*, 881–884.
- (20) Gjoni, T.; Urwyler, S. Receptor activation involving positive allosteric modulation, unlike full agonism, does not result in GABAB receptor desensitization. *Neuropharmacology* **2008**, *55*, 1293–1299.
- (21) Trabanco, A. A.; Cid, J. M.; Lavreysen, H.; Macdonald, G. J.; Tresadern, G. Progress in the development of positive allosteric modulators of the metabotropic glutamate receptor 2. *Curr. Med. Chem.* **2011**, *18*, 47–68.
- (22) Trabanco, A. A.; Cid, J. M. mGluR2 positive allosteric modulators (PAMs): a patent review (2009–present). *Expert Opin. Ther. Patents* **2013**, *23*, 629–647.
- (23) Lorrain, D. S.; Schaffhauser, H.; Campbell, U. C.; Baccei, C. S.; Correa, L. D.; Rowe, B.; Rodriguez, D. E.; Anderson, J. J.; Varney, M. A.; Pinkerton, A. B.; Vernier, J.-M.; Bristow, L. J. Group II mGlu receptor activation suppresses norepinephrine release in the ventral hippocampus and locomotor responses to acute ketamine challenge. *Neuropsychopharmacology* **2003**, *28*, 1622–1632.
- (24) Johnson, M. P.; Baez, M.; Jagdmann, G. E.; Britton, T. C.; Large, T. H.; Callagaro, D. O.; Tizzano, J. P.; Monn, J. A.; Schoepp, D. D. Discovery of allosteric potentiators for the metabotropic glutamate 2 receptor: synthesis and subtype selectivity of N-(4-(2-methoxyphenoxy)phenyl)-N-(2,2,2-trifluoroethylsulfonylethyl)pyrid-3-ylmethylamine. *J. Med. Chem.* **2003**, *46*, 3189–3192.
- (25) Pinkerton, A. B.; Vernier, J.-M.; Schaffhauser, H.; Rowe, B. A.; Campbell, U. C.; Rodriguez, D. E.; Lorrain, D. S.; Baccei, C. S.; Daggett, L. P.; Bristow, L. J. Phenyl-tetrazolyl acetophenones: discovery of positive allosteric potentiators for the metabotropic glutamate 2 receptor. *J. Med. Chem.* **2004**, *47*, 4595–4599.
- (26) Fell, M. J.; Witkin, J. M.; Falcone, J. F.; Katner, J. S.; Perry, K. W.; Hart, J.; Rorick-Kehn, L.; Overshiner, C. D.; Rasmussen, K.; Chaney, S. F.; Benvenga, M. J.; Li, X.; Marlow, D. L.; Thompson, L. K.; Lueck, S. K.; Wafford, K. A.; Seidel, W. F.; Edgar, D. M.; Quests, A. T.; Felder, C. C.; Wang, X.; Heinz, B. A.; Nikolayev, A.; Kuo, M. S.; Mayhugh, D.; Khilevich, A.; Zhang, D.; Ebert, P. J.; Eckstein, J. A.; Ackermann, B. L.; Swanson, S. P.; Catlow, J. T.; Dean, R. A.; Jackson, K.; Tauscher-Wisniewski, S.; Marek, G. J.; Schkeryantz, J. M.; Svensson, K. A. N-(4-((2-(Trifluoromethyl)-3-hydroxy-4-(isobutyryl)-phenoxy)methyl) benzyl)-1-methyl-1H-imidazole-4-carboxamide (THIC), a novel metabotropic glutamate 2 potentiator with potential anxiolytic/antidepressant properties: in vivo profiling suggests a link between behavioral and central nervous system neurochemical change. *J. Pharmacol. Exp. Ther.* **2011**, *336*, 165–177.
- (27) Johnson, P. L.; Fitz, S. D.; Engleman, E. A.; Svensson, K. A.; Schkeryantz, J. M.; Shekhar, A. Group II metabotropic glutamate receptor type 2 allosteric potentiators prevent sodium lactate-induced panic-like response in panic-vulnerable rats. *J. Psychopharmacol.* **2013**, *27*, 152–61.
- (28) Cid, J. M.; Duvey, G.; Cluzeau, P.; Nhem, V.; Macary, K.; Raux, A.; Poirier, N.; Muller, J.; Bolea, C.; Finn, T.; Urios, L.; Epping-Jordan, M.; Chamelot, E.; Derouet, F.; Girard, F.; MacDonald, G. J.; Vega, J. A.; de Lucas, A. I.; Matesanz, E.; Lavreysen, H.; Linares, M. L.; Oehlich, D.; Oyarzabal, J.; Tresadern, G.; Trabanco, A. A.; Andres, J. I.; Le Poul, E.; Imogai, H.; Lutjens, R.; Rocher, J.-P. Discovery of 1,5-disubstituted pyridones: a new class of positive allosteric modulators of the metabotropic glutamate 2 receptor. *ACS Chem. Neurosci.* **2010**, *1*, 788–795.
- (29) Cid, J. M.; Duvey, G.; Tresadern, G.; Nhem, V.; Funary, R.; Cluzeau, P.; Vega, J. A.; de Lucas, A. I.; Matesanz, E.; Alonso, J. M.; Linares, M. L.; Andres, J. I.; Poli, S.; Lutjens, R.; Imogai, H.; Rocher, J.-P.; MacDonald, G. J.; Oehlich, D.; Lavreysen, H.; Ahnaou, A.; Drinkenburg, W.; Mackie, C.; Trabanco, A. A. Discovery of 1,4-disubstituted 3-cyano-2-pyridones: a new class of positive allosteric modulators of the metabotropic glutamate 2 receptor. *J. Med. Chem.* **2012**, *55*, 2388–2405.
- (30) Tresadern, G.; Cid, J. M.; MacDonald, G. J.; Vega, J. A.; de Lucas, A. I.; Garcia, A.; Matesanz, E.; Linares, M. L.; Oehlich, D.; Lavreysen, H.; Biesmans, I.; Trabanco, A. A. Scaffold hopping from pyridones to imidazo[1,2-a]pyridines. new positive allosteric modulators of metabotropic glutamate 2 receptor. *Bioorg. Med. Chem. Lett.* **2010**, *20*, 175–179.
- (31) Trabanco, A. A.; Tresadern, G.; MacDonald, G. J.; Vega, J. A.; de Lucas, A. I.; Matesanz, E.; Garcia, A.; Linares, M. L.; Alonso de Diego, S. A.; Alonso, J. M.; Oehlich, D.; Ahnaou, A.; Drinkenburg, W.; Mackie, C.; Andres, J. I.; Lavreysen, H.; Cid, J. M. Imidazo[1,2-a]pyridines: orally active positive allosteric modulators of the metabotropic glutamate 2 receptor. *J. Med. Chem.* **2012**, *55*, 2688–2701.
- (32) Cid, J. M.; Tresadern, G.; Vega, J. A.; de Lucas, A. I.; Matesanz, E.; Iturrino, L.; Linares, M. L.; Garcia, A.; Andres, J. I.; MacDonald, G. J.; Oehlich, G.; Lavreysen, H.; Megens, A.; Ahnaou, A.; Drinkenburg, W.; Mackie, C.; Pype, S.; Gallacher, D.; Trabanco, A. A. Discovery of 3-cyclopropylmethyl-7-(4-phenylpiperidin-1-yl)-8-trifluoromethyl-1,2,4-triazolo[4,3-a]pyridine (JNJ-42153605): a positive allosteric modulator of the metabotropic glutamate 2 receptor. *J. Med. Chem.* **2012**, *55*, 8770–8789.
- (33) Kent, J.; Anghelescu, I.-G.; Kezic, I.; Daly, E.; Ceusters, M.; De Smedt, H.; Van Nueten, L.; De Boer, P. *Safety, tolerability and potential therapeutic efficacy of a novel glutamate modulator as adjunctive treatment in patients with schizophrenia*, 166th Annual Meeting of the American Psychiatric Association, San Francisco, CA, May 18–22, 2013; Abstract, 3160-P.
- (34) Investigation of the safety, tolerability and potential therapeutic effects of JNJ-40411813 in patients with schizophrenia. <http://clinicaltrials.gov/show/NCT01323205>.
- (35) Hopkins, C. R. Is there a path forward for mGlu2 positive allosteric modulators for the treatment of schizophrenia? *ACS Chem. Neurosci.* **2013**, *4*, 211–213.
- (36) AstraZeneca 2010 financial results. <http://www.astrazeneca.com/Investors/financial-information/Financial-results/2010-Financial-results>.
- (37) Litman, R. E.; Smith, M. A.; Doherty, J.; Cross, A.; Raines, S.; Zukin, S. AZD8524, a positive allosteric modulator at the mGluR2 receptor, does not improve symptoms in schizophrenia: a proof of principle study, 53rd NCDEU: an annual meeting sponsored by ASCP, Hollywood, Florida, May 28–31, 2013; Poster 83.
- (38) Addex reports top-line data from a successful phase 2a clinical study with ADX71149 in schizophrenia patients. <http://www.addextherapeutics.com/investors/press-releases/news-details/article/>

addex-reports-top-line-data-from-a-successful-phase-2a-clinical-study-with-adx71149-in-schizophrenia/.

(39) Lavreysen, H. *Discovery and early clinical development of novel mGlu2 receptor PAMs*, American College of Neuropsychopharmacology 52nd Annual Meeting, Hollywood, Florida, Dec 8–12, 2013.

(40) A study of JNJ-40411813 as supplementary treatment to an antidepressant in adults with depression and anxiety symptoms. <http://clinicaltrials.gov/show/NCT01582815>.

(41) Addex Reports top-line data from ADX71149 phase 2a study in patients with major depressive disorder (MDD) with significant anxiety symptoms. <http://www.addextherapeutics.com/investors/press-releases/news-details/article/addex-reports-top-line-data-from-adx71149-phase-2a-study-in-patients-with-major-depressive-disorder/>.

(42) Cid-Nuñez, J. M.; Trabanco-Suarez, A. A.; Macdonald, G. J.; Duvey, G. A. J.; Lütjens, R. J. *Preparation of 1,4-disubstituted 3-cyanopyridone derivatives as positive mGluR2 receptor modulators*. WO/2008/107480, 2008.

(43) Cid-Nuñez, J. M.; Trabanco-Suárez, A. A.; Macdonald, G. J.; Duvey, G. A. J.; Lütjens, R. J. *Preparation of 3-cyano-4-(4-phenylpiperidin-1-yl)-pyridin-2-one derivatives for treating and preventing neurological and psychiatric diseases associated with glutamate dysfunction*. WO/2008/107479, 2008.

(44) Cid-Nuñez, J. M.; Trabanco-Suárez, A. A.; Macdonald, G. J.; Duvey, G. A. J.; Lütjens, R. J.; Finn, T. P. *Preparation of bipyridinones as positive allosteric modulators of mGluR2 for treating neurological and psychiatric disorders*. WO/2009/033704, 2009.

(45) The in vitro [³⁵S]GTPγS assay provides two measures of compound activity: pEC₅₀, which is defined as the negative logarithm of the concentration at which half-maximal potentiation of glutamate is reached, and the maximal increase in observed glutamate response, the % E_{MAX}.

(46) Compound 6 was incubated with human and rat liver microsomes at 0.4% final solvent concentration (0.16% DMSO and 0.24% CH₃CN). The study was conducted to identify the main metabolites formed after 0 min (control) and 60 min of incubation time in the presence of an NADPH generating system at 37 °C. Test concentration of 6 was 5 μM. Samples were compared to the control incubations in which compound was added at termination. Data were acquired on a Waters UPLC/QToF Premier mass spectrometer using a 10 min generic UPLC method and a generic MSe method. Complementary MS/MS experiments were performed when necessary. An Acquity UPLC C18 (2.1 mm × 100 mm, 1.8 μm) column was used. Interpretation of data was performed with Waters Metabolynx software.

(47) Lavreysen, H.; Langlois, X.; Ahnaou, A.; Drinkenburg, W.; te Riele, P.; Biesmans, I.; Van der Linden, I.; Peeters, L.; Megens, A.; Wintmolders, C.; Cid, J.; Trabanco, A. A.; Andres, I.; Dautzenberg, F. M.; Lütjens, R.; Macdonald, G.; Atack, J. R. Pharmacological characterization of JNJ-40068782, a new potent, selective and systemically active positive allosteric modulator of the mGlu2 receptor and its radioligand [³H]JNJ-40068782. *J. Pharmacol. Exp. Ther.* **2013**, *346*, 514–527.

(48) Feinberg, I.; Campbell, I. G.; Schoepp, D. D.; Anderson, K. The selective group mGlu2/3 receptor agonist LY379268 suppresses REM sleep and fast EEG in the rat. *Pharmacol., Biochem. Behav.* **2002**, *73*, 467–74.

(49) Ahnaou, A.; Dautzenberg, F. M.; Geys, H.; Imogai, H.; Gibelin, A.; Moechars, D.; Steckler, T.; Drinkenburg, W. H. Modulation of group II metabotropic glutamate receptor (mGlu2) elicits common changes in rat and mice sleep–wake architecture. *Eur. J. Pharmacol.* **2009**, *603*, 62–72.

(50) Compound 36 was tested for agonist or antagonist activity on mGlu receptors in fluorescent Ca²⁺ assays using HEK293 cells expressing human mGlu1, mGlu3, and mGlu5 receptors or [³⁵S]GTPγS assays using L929 cells expressing human mGlu4 or CHO cells expressing rat mGlu6 receptors.

(51) The CEREP selectivity screen was performed on the following targets: 5HT1A, 5HT2A, 5HT3, 5HT5A, 5HT6, 5HT7, A1, A2A, A3, AT1, Beta1, BK2, CCKA, CCR1, D1, D2, DAT, ETA, GAL2, H1, H2,

IL8B, CXCR2, M1, M2, M3, MC4, NET, NK2, NK3, NPY1, NPY2, NT1, OP1, OP3, ORL1, V1A, VIP, SST, 5HT1B, α1, α2, BZD, CaCH, CICH, GABA, KCH, NaCH, and SKCaCH.